

RESEARCH ARTICLE

Nutrient and sediment loading affect multiple facets of functionality in a tropical branching coral

Danielle M. Becker* and Nyssa J. Silbiger*

ABSTRACT

Coral reefs, one of the most diverse ecosystems in the world, face increasing pressures from global and local anthropogenic stressors. Therefore, a better understanding of the ecological ramifications of warming and land-based inputs (e.g. sedimentation and nutrient loading) on coral reef ecosystems is necessary. In this study, we measured how a natural nutrient and sedimentation gradient affected multiple facets of coral functionality, including endosymbiont and coral host response variables, holobiont metabolic responses and percent cover of Pocillopora acuta colonies in Mo'orea, French Polynesia. We used thermal performance curves to quantify the relationship between metabolic rates and temperature along the environmental gradient. We found that algal endosymbiont percent nitrogen content, endosymbiont densities and total chlorophyll a content increased with nutrient input, while endosymbiont nitrogen content per cell decreased, likely representing competition among the algal endosymbionts. Nutrient and sediment loading decreased coral metabolic responses to thermal stress in terms of their thermal performance and metabolic rate processes. The acute thermal optimum for dark respiration decreased, along with the maximal performance for gross photosynthetic and calcification rates. Gross photosynthetic and calcification rates normalized to a reference temperature (26.8°C) decreased along the gradient. Lastly, percent cover of P. acuta colonies decreased by nearly two orders of magnitude along the nutrient gradient. These findings illustrate that nutrient and sediment loading affect multiple levels of coral functionality. Understanding how local-scale anthropogenic stressors influence the responses of corals to temperature can inform coral reef management, particularly in relation to the mediation of land-based inputs into coastal coral reef ecosystems.

KEY WORDS: Nutrient loading, Sediment loading, Pocillopora acuta, Thermal performance curve, Land-based inputs, Coral physiology

INTRODUCTION

Coral reef ecosystems are some of the most biodiverse habitats in the world, providing ecological and economic services worldwide (Burke et al., 2011; Speers et al., 2016; Hughes et al., 2017; Cowburn, et al., 2018). Reef-building corals (scleractinians) create the three-dimensional reef structure that provides habitat for millions of species and protects the shorelines of coastal communities (Bellwood and Hughes, 2001; Hughes et al., 2018). Yet, local and global anthropogenic stressors are rapidly

Department of Biology, California State University, Northridge, CA 91330, USA.

*Authors for correspondence (danielle.becker.927@my.csun.edu; nyssa.silbiger@csun.edu)

D.M.B., 0000-0002-2710-9175; N.J.S., 0000-0003-4916-3217

diminishing the biodiversity and structural complexity of coral reefs (De'ath et al., 2012; Hobday et al., 2016; Hughes et al., 2018). In the past 30–50 years, it is estimated that coral cover on reefs has declined by at least 50% in some of the world's largest tropical regions (Bruno and Selig, 2007; Hoegh-Guldberg et al., 2007; De'ath et al., 2012). Thermal stress linked to global climate change is considered to be one of the main causes of coral reef decline over the last century (van Hooidonk et al., 2013; Hoegh-guldberg et al., 2017; Hughes et al., 2018). Secondary to ocean warming, local anthropogenic stressors, such as nutrient loading and sedimentation, pose threats to corals by shifting the competitive dominance of reef organisms towards macroalgae (Littler and Littler, 1984; Burkepile and Hay, 2006; Hughes et al., 2007) and increasing the susceptibility of corals to bleaching events (Halpern et al., 2008; Carilli et al., 2009; Vega Thurber et al., 2014; Rosset et al., 2017; Burkepile et al., 2019; Donovan et al., 2020). As global- and localscale anthropogenic stressors become more intense (Hoegh-Guldberg et al., 2007), it is necessary to better understand the ecological ramifications of both warming and land-based inputs on scleractinian corals.

The separate effects of warming and land-based inputs on coral physiology have been extensively studied (Fabricius, 2005; Edmunds et al., 2011; Putnam and Edmunds, 2011; Putnam and Gates, 2015; Hoegh-Guldberg et al., 2017; McCulloch et al., 2017; Hughes et al., 2017; Wall et al., 2019). Severe bleaching events caused by ocean warming negatively affect the metabolic response of corals (Putnam and Edmunds, 2011; Gibbin et al., 2014; Hughes et al., 2017; Wall et al., 2018), reduce individual and community calcification rates (De'ath et al., 2009; DeCarlo et al., 2017), and make corals more susceptible to infectious diseases (Harvell et al., 2002; Rosenberg and Ben-haim, 2002; Bruno et al., 2007). More recently, marine heatwaves (severe acute warming events) have been shown to accelerate calcium carbonate dissolution and coral colony mortality, inducing rapid coral skeletal decay (Leggat et al., 2019). Furthermore, excessive nutrient and sediment loading from terrestrial environments lower photosynthetic efficiency in the endosymbionts (Dubinsky et al., 1990), reduce skeletal extension and linear extension rates of coral colonies (Dunn et al., 2012; Lubarsky et al., 2018; Baumann et al., 2019), increase bioerosion/ dissolution rates on reefs (Lubarsky et al., 2018; Silbiger et al., 2018), and cause a loss in net calcification rates of reef communities (Silbiger et al., 2018).

Nutrient loading has also been shown to have positive effects on corals, in certain conditions, by increasing coral growth rates (Koop et al., 2001; Bongiorni et al., 2003; Dunn et al., 2012) and reducing the susceptibility of corals to bleaching (McClanahan et al., 2003). Further, reduced UV exposure attributed to sediment loading has been associated with reduced bleaching in corals found in Palau (Van Woesik et al., 2012), Barbados (Oxenford and Vallès, 2016) and Columbia (Bayraktarov et al., 2013). The ability for coral reefs to exist over a wide range of nutrient and sediment conditions

List of symbols and abbreviations Akaike information criterion ATP metabolic energy (adenosine triphosphate) $b(T_c)$ metabolic rate normalized to a reference temperature $(\mu mol cm^{-2} h^{-1})$ Ca²⁺ calcium ions CCA crustose coralline algae CRM certified reference material CT_{max} critical thermal maximum CT_{min} critical thermal minimum DIN:DIP dissolved inorganic nitrogen-to-phosphorus ratios E_{a} activation energy (eV) deactivation energy (eV) E_{h} FW freshwater GP gross photosynthesis (μmol cm⁻² h⁻¹) HgCl₂ mercuric chloride saturating light (µmol photons m⁻² s⁻¹) I_{k} sum of the percentile-ranks of the Z_{min} scores for each L_{pc} component metric Ν nitrogen NC net light calcification (μmol cm⁻² h⁻¹) NH_4 ammonium (µmol I-1) nitrite (µmol I⁻¹) NO_2 nitrate (µmol I⁻¹) NO_3 NP net photosynthesis PAR photosynthetically active radiation **PFD** photon flux density (µmol photons m⁻² s⁻¹) P_{max} area-based gross photosynthetic rate (μmol cm⁻² h⁻¹) area-based net photosynthetic rate (μmol cm⁻² h⁻¹) PO₄3 phosphate (µmol l⁻¹) dark respiration (μmol cm⁻² h⁻¹) R_{d} SA the surface area of the coral samples determined by the paraffin wax-dipping technique (cm²) incubation time (h) TA total alkalinity T_{opt} acute thermal optimum (°C) **TPC** thermal performance curve University of California, Berkeley Richard B. Gump **UCB Gump** Station South Pacific Research Station UCSB MSI University of California, Santa Barbara Marine Science Institute volume of water in the experimental aquaria (chambers) (cm³) ΛTA difference between the initial pre-incubation and postincubation TA value (μmol kg⁻¹) curvature parameter, dimensionless Θ maximal rate of performance (μmol cm⁻² h⁻¹) μ_{max} density of seawater (g cm⁻³) σ apparent quantum yield (AQY) φ

throughout geographic ranges complicates our understanding of how eutrophication and sedimentation influence coral functionality.

Less is known about how land-based inputs and ocean warming interact to affect coral physiology (but see Faxneld et al., 2010; Burkepile et al., 2019). Some studies have found that nutrient enrichment and increased sedimentation rates can exacerbate the negative effects of elevated thermal stress on corals (Wooldridge, 2009; Wiedenmann et al., 2013; Serrano et al., 2018; Hadjioannou et al., 2019). For example, the influx of suspended material coupled with increasing temperatures causes oxidative stress in the coral holobiont, overwhelming oxygen handling mechanisms for oxygen radicals (superoxides and peroxides), which can directly damage cellular components that corals rely on for growth and productivity (Fabricius, 2005; Cunning et al., 2017; Humanes et al., 2017). Furthermore, varying types of nutrient enrichment (i.e. coastal

runoff, sewage, agriculture) impact the severity and prevalence of coral bleaching (Cunning and Baker, 2013; Burkepile et al., 2019; Donovan et al., 2020). A study found that bleaching prevalence (the proportion of colonies that had any amount of bleached tissue) in ~3000 *Acropora* spp. and *Pocillopora* spp. coral colonies increased by 100% and 60% at sites with nutrient diffusers, respectively, when compared with control corals (Burkepile et al., 2019). Their results indicate that anthropogenic nutrient enrichment could lower the thermal bleaching threshold for corals, highlighting the importance of examining both local and global stressors in concert. However, we still lack a mechanistic understanding of the interactive effects of local and global stressors on several other coral physiological processes in addition to bleaching.

Metabolic processes such as photosynthesis, respiration and calcification are important indicators of organismal health and are continuously being altered by organisms to adjust their physiological mechanisms in varying environments. byproducts (i.e. sugars, lipids, proteins, fixed carbon) produced through photosynthesis by the algal endosymbionts, that are translocated to the coral host, are mostly consumed by the respiration processes occurring in the coral holobiont, i.e. the coral animal and its associated microorganisms consisting of bacteria, archaea, fungi, viruses and protists (Rohwer et al., 2002). Respiration is a metabolic pathway that includes the TCA cycling process in the coral holobiont, resulting in the production of metabolic energy (ATP), which is used for all energy-requiring processes, along with the transport of calcium ions (Ca²⁺) from surrounding seawater to the skeleton for calcification (Al-Horani et al., 2002). Calcification and dissolution rates on coral reefs are closely related to fluctuations in photosynthetic and respiration rates occurring at the reef scale that modify the local pH environment (Silverman et al., 2007; Silbiger et al., 2014, 2018). Because these metabolic processes respond differently to environmental stressors (i.e. temperature and land-based inputs) (Al-Horani, 2005; Bahr et al., 2018; Courtial et al., 2018; Silbiger et al., 2018, 2019; Morris et al., 2019), it is important to compare multiple metabolic processes to understand how coral physiology will be affected on future coastal coral reef ecosystems.

Thermal performance curves (TPCs) are commonly used as a mechanistic approach to compare thermal performance among different ectothermic species (Dell et al., 2011; Sinclair et al., 2012; Bestion et al., 2018), and in populations living with different thermal histories (Angilletta, 2009; Andrews and Schwarzkopf, 2012), altered environmental conditions (Bestion et al., 2018; Kellermann et al., 2019) and in different geographic ranges (Angilletta, 2009; Sgrò et al., 2010; Aichelman et al., 2019; Jurriaans and Hoogenboom, 2019; Silbiger et al., 2019). TPCs are reaction norms that describe the relationship between a continuous environmental variable (e.g. temperature) and a continuous phenotypic variable in ectothermic species (Angilletta, 2009; Schulte et al., 2011; Sinclair et al., 2016). Therefore, a TPC approach could help uncover how local stressors affect thermal performance in corals. There are several metrics that can be derived from TPCs, which include: critical thermal minimum (CT_{min}) and critical thermal maximum (CT_{max}) – which mark the full range of the organism's thermal tolerance (breadth) – thermal optimum of the performance measure (T_{opt}) , maximal rate of performance (μ_{max}) and metabolic rate normalized to a reference temperature $[b(T_c)]$, which is often used to compare rates between organisms or functions (Huey and Stevenson, 1979; Huey and Kingsolver, 1989; Angilletta., 2009; Latimer et al., 2011; Tattersall et al., 2012; Padfield et al., 2015; Schaum et al., 2017; Silbiger et al., 2019).

Furthermore, the sensitivity of the response variable is shown by TPCs through the rates of activation ($E_{\rm a}$) and deactivation ($E_{\rm h}$) energy that are derived from the positive and negative slopes on either side of $T_{\rm opt}$. An organism's phenotypic plasticity or adaptive evolutionary traits can modify a TPC by altering the breadth (width of the curve), $T_{\rm opt}$ (horizontal shift of the curve) or $\mu_{\rm max}$ (vertical shift of the curve) (Angilletta et al., 2004). Therefore, TPC metrics can be used to understand how the measures of the thermal performance of corals may shift in response to a natural gradient of nutrient and sediment loading.

Here, we measured how nutrient and sediment loading affect multiple facets of coral functionality in Pocillopora acuta colonies along the north-shore fringing reefs in Mo'orea, French Polynesia. The overarching goal was to investigate how natural variation in nutrient and sediment loading influences (1) endosymbiont and coral host response variables, (2) holobiont metabolic response variables and thermal performance metrics $[T_{opt}, \mu_{max} \text{ and } b(T_c)]$ for gross photosynthesis (GP), dark respiration (R_d) and net light calcification (NC), and (3) percent cover of *P. acuta* colonies. Based on what is known about coral-algal symbiosis dynamics (Cunning and Baker, 2013; Muller-Parker et al., 2015; Cunning et al., 2017), we hypothesized that elevated nutrients would increase endosymbiont densities and chlorophyll a content, but compromise host performance when exposed to thermal stress (Wiedenmann et al., 2013; Kitchen et al., 2020). Because nutrient and sediment loading have been found to negatively impact coral functionality (Rogers, 1990; Fabricius, 2005), we hypothesized that T_{opt} , metabolic rate processes (GP, R_d , NC), performance measures $[\mu_{max}, b(T_c)]$, and percent cover would decrease with elevated nutrient and sediment loading. These combined data show that local-scale stressors affecting coral organismal physiology may lead to changes in percent cover, which has implications for how population structure and ecosystem function on coral reefs will respond to future climatic conditions.

MATERIALS AND METHODS Study sites and coral collection

Colonies of Pocillopora acuta Lamarck 1816 (n=54) were collected between 0.5 and 1 m depth from six locations (n=9 colonies per location) that exhibited a gradient in nutrient loading and sedimentation rates along north-shore fringing reefs in Mo'orea, French Polynesia, during the Austral winter of 2019 (Fig. 1A). Fringing reef sites along the north-shore lagoonal habitats are shallow water reef communities that are sheltered from waves and oceanic swell, typically found within 100 m of the shoreline from depths between 0 and 3 m. Populations of our focal branching coral species, *P. acuta*, are typically found in shallow waters (<4 m depth) (Fong et al., 2019) and are widely distributed across Indo-Pacific reefs (Schmidt-Roach et al., 2014; Poquita-Du et al., 2017; Torres and Ravago-Gotanco, 2018). In response to environmental change, P. acuta colonies are hypothesized to allocate more energy to growth than to survival responses (Pinzón et al., 2014) owing to their weedy life-history strategy (Darling et al., 2012, 2013).

Sample sizes of P. acuta were based on preliminary data collected in January 2019 that showed an n of 8 elicited an effect while also minimizing damage to the reef (D. M. Becker, unpublished data). To ensure that all samples could be processed in the same photoperiod, we separated the six sites into three paired blocks so that TPC trials (which take \sim 12 h) could include four fragments from each paired site. The three paired site blocks were along the north-shore fringing reef sites for sample collection (western: $17^{\circ}29'33.684''S$, $149^{\circ}52'6.852''W$, $17^{\circ}29'25.152''S$, $149^{\circ}51'$

1.008"W; central: 17°29'4.632"S, 149°50'23.064"W, 17°29' 5.532"S, 149°50'43.872"W; and eastern: 17°28'51.0"S, 149°48' 17.8"W, 17°28'45.588"S, 149°47'33.792"W) (Fig. 1A).

Pocillopora acuta colonies were removed from the reef with a hammer and chisel on snorkel, placed in clean ziplock bags full of seawater, and transported to the University of California, Berkeley, Richard B. Gump South Pacific Research Station (UCB Gump Station) in a seawater-filled cooler and immediately placed in flowthrough seawater tables before being fragmented. Using a stainlesssteel diagonal cutter, we cut each colony into four or five multibranch fragments (7.8×7.8 cm), which were measured using calipers. Two of the designated fragments were used for light and dark respirometry trials. The other two fragments were used for endosymbiont and coral host response variables including chlorophyll a content, endosymbiont densities, endosymbiont % nitrogen (N) content, endosymbiont N content cell⁻¹, tissue biomass, and coral tissue % N content. A fifth fragment was randomly selected from four colonies per location and used to determine saturating light conditions for the corals. The two fragments delegated for endosymbiont and coral host response variables (one for % tissue N and one for the remaining parameters) were immediately frozen at -20° C until processing. The two fragments designated for photosynthesis, respiration calcification trials were affixed to pre-labeled acrylic coral plugs (Industry, CA, USA) using hot glue around the base of the coral skeleton while the fragment was submerged. After coral fragments were affixed, they were deployed in situ to recover from the fragmentation process at their origin reef site for 7–14 days. The coral plugs were placed in individual holes on a constructed acrylic sheet with an O-ring placed around the bottom of the plug for stabilization. Each acrylic plate had a cage surrounding it made of 2 cm wide Gutter Guard Mesh (Hallandale, FL, USA) to prevent corallivory. Coral samples were again collected around sunset, \sim 12 h before each photosynthesis or dark respiration trial, and held in an ambient seawater flow-through system at the UCB Gump Station. The coral samples designated for the dark respiration trials were kept in darkness by wrapping a thick black plastic bag around each tank for ~ 11 h prior to measuring dark respiration, while the coral samples for photosynthesis trials were kept in natural light under a shade.

Research was completed under permits issued by the French Polynesian Government (Délégation à la Recherche) and the Hautcommissariat de la République en Polynésie Française (DTRT) (Protocole d'Accueil 2005-2019).

Site characteristics

Sedimentation rates

Sediment traps (n=3) were deployed in triplicate for ~72 h at each of the six sites during the coral recovery period. Traps were constructed with six individual 6×30 cm (diameter×height) PVC pipes (Storlazzi et al., 2011) that each had a 2×4 cm (diameter×height) PVC pipe glued to its side. The smaller PVC pipe slid over an 8-inch long screw that was installed into a cement base. Sediment traps were recovered *in situ* by wrapping the opening of the PVC pipe with parafilm before removal from the reef. The sediment samples were brought back to the laboratory, where the volume of the sediment sample was measured and filtered through a pre-weighed 1 μ m pore size, 47 mm Whatman® polycarbonate filter (Maidstone, UK). The filters were dried in an oven (Fisher Scientific Isotemp Oven, Waltham, MA, USA) at 80°C for 24 h (Lozano-Cortés et al., 2014). Each sample was weighed to the nearest 0.001 g on an analytical balance to obtain dry mass and normalized to the open

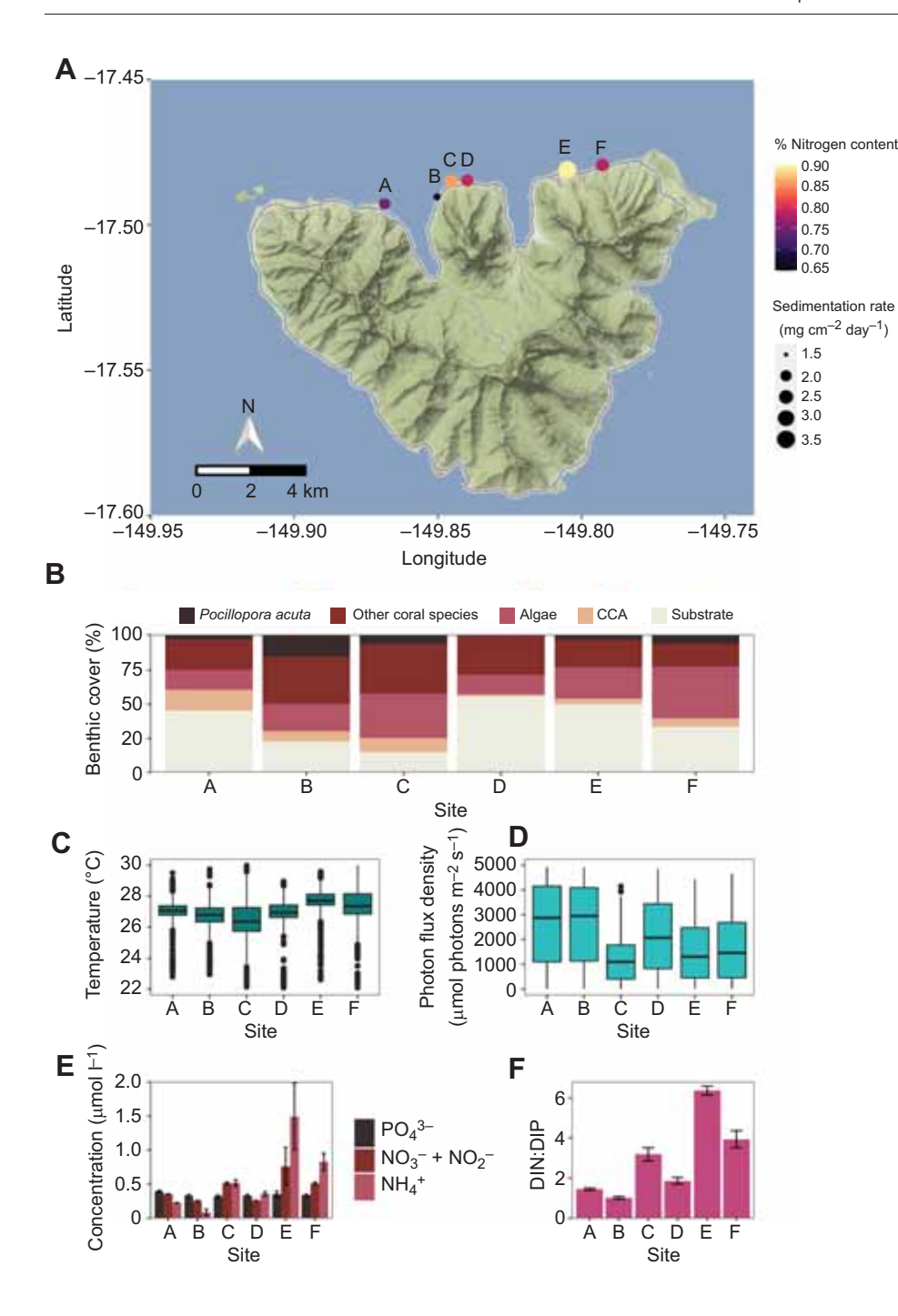


Fig. 1. Map and accompanying environmental, physical and biological characteristics of six north-shore fringing reef sites (sites A-F) across Mo'orea, French Polynesia. (A) The size of the points represents the sedimentation rate (mg cm⁻² day⁻¹) at each site, while the color gradient represents the mean % tissue N of Turbinaria ornata (n=3) at each site from low (black) to high (yellow). (B) Benthic cover is the total percent cover of the benthic community for our study species Pocillopora acuta, other coral species (23 coral genera), total algae (macroalgae, turf and fleshy algae), crustose coralline algae (CCA) and substrate (bare rock, rubble, sand and/or bare space). (C) Temperature (°C) and (D) daytime photon flux density (µmol photons m⁻² s⁻¹) were measured over a 14 day deployment; the median (line within box), first and third quartiles (box), non-outlier range (whiskers) and outliers (dots) are shown. (E) Mean (±s.e.m.) PO₄³⁻, $NO_3^- + NO_2^-$, and NH_4^+ (µmol I^{-1}) concentrations and (F) DIN $(NO_3^- + NO_2^- + NH_4^+)$:DIP (PO_4^{3-}) ratios are shown across sites. The water column nutrient data were obtained from water samples (n=2 per site).

area of the trap (mg $\rm cm^{-2}~day^{-1}$) (Storlazzi et al., 2011; Lozano-Cortés et al., 2014).

Algal tissue nitrogen sampling and water column nutrients

Macroalgal % tissue N content is an integrated measure of nutrient loading for each site (Fong et al., 1994; Lin and Fong, 2008) (Fig. 1A). Percent tissue N content for *Turbinaria ornata* was calculated from replicate individuals (*n*=3) per site at the same time the corals were collected for fragmentation. Samples were returned to the laboratory and approximately 1 g (wet mass) of tissue was removed (5 cm from a branch apex) from each individual, rinsed in freshwater (FW), where epiphytes were removed manually with forceps, and dried to constant mass at 80°C (Carpenter, 2019). Dried samples were processed for CHN analysis by the means of

high-temperature (1000°C) combustion following the Dumas method (Shea and Watts, 1939) of samples in an oxygen-enriched helium atmosphere in an elemental analyzer (Control Equipment Corporation, Model CEC 440HA, North Chelmsford, MA, USA) at the University of California, Santa Barbara Marine Science Institutes (UCSB MSI) Analytical Lab. We also collected water column samples to characterize nutrient concentrations in the seawater at the time of collection. Two replicate water samples were collected from the benthos using 60 ml lip-lok tip syringes for dissolved inorganic nitrate (NO₃⁻)+nitrite (NO₂⁻), ammonium (NH₄⁺) and phosphate (PO₄³⁻). The samples were filtered through a 0.7 μ m GF/F filter (Whatman) and the seawater samples were placed in a -20°C freezer immediately upon returning to the UCB Gump Station for later analysis at the UCSB MSI Analytical Lab.

Dissolved inorganic nutrients (PO₄³⁻, NO₃⁻+NO₂⁻, NH₄⁺) were analyzed using flow injection (QuikChem 8500 Series 2, Lachat Instruments, Zellweger Analytics, Inc., Loveland, CO, USA) at the UCSB MSI Analytical Lab (Johnson et al., 1985).

Temperature and light

Temperature, accuracy $\pm 0.21^{\circ}\text{C}$ from 0°C to 50°C, and light intensity, accuracy $\pm 10\%$ from 0 to 167,731 lux, were recorded *in situ* at all sites with HOBO® loggers (Onset® HOBO® TidbiT® v2 Temp Data Logger UTBI-001 and Onset® HOBO® Pendent Light Intensity Data Logger MX2202, respectively; Bourne, MA, USA) every 15 min during the 7–14 day recovery period. Light loggers were cable-tied to a small acrylic slate before deployment to ensure that the loggers were orientated at a 180-deg angle facing upward and would stay affixed during the experimental period. The light intensity data were converted from luminous flux (lux) to photon flux density (PFD) of photosynthetically active radiation (PAR) [µmol photons m⁻² s⁻¹] using an exponential decay fit [PAR_{LICOR}= A_1 e(-HOBO/ t_1)+ y_0], following methods by Long et al. (2012) to obtain relative values across all sites.

Endosymbiont and coral host response variablesTissue removal

Tissue was removed from the frozen coral skeleton using an Iwata Eclipse HP-BCS airbrush (Portland, OR, USA) filled with filtered seawater (0.2 µm). Each of the resulting coral tissue slurries was individually homogenized with an electric hand-held homogenizer (BT Lab Systems, St Louis, MO, USA) for 15 s at 3000 rpm, and aliquots were taken for each endosymbiont and coral host response variable (chlorophyll a content, endosymbiont densities, endosymbiont % N content, endosymbiont N content cell⁻¹, tissue biomass and coral tissue % N content) (Wall et al., 2017). The aliquots for each parameter were frozen at -20° C until analysis. The coral skeletons were placed in a drying oven (Fisher Scientific Isotemp Oven) at 60°C for 4 h before surface area measurements were taken. Before obtaining estimates of surface area for the P. acuta fragments, we used pre-weighed wooden dowels of known surface areas to create a standard curve of mass change of wax dipped dowels against geometrically calculated surface area, with an $R^2>0.9$ for the relationship, following methods from Stimson and Kinzie (1991). The dried coral fragment surface areas were measured by first weighing the coral skeleton before dipping them into a 65°C Minerva paraffin wax bath (Monroe, GA, USA) for 2 s, before removal and then quickly rotating the coral skeleton in the air at a standardized rate (10 revolutions over 2 s). The coral skeletons were then cooled for 10 min before their final mass (g) was measured. The established calibration curve was then used to determine their surface area (cm⁻²) (Stimson and Kinzie, 1991; Veal et al., 2010).

Algal endosymbiont densities

To quantify algal endosymbiont densities, repeated cell counts (n=6-8) were conducted for aliquoted (1 ml) coral tissue slurry samples (n=54) using an Improved Neubauer Haemocytometer (Marienfeld Superior, Lauda-Königshofen, Germany). The endosymbiont cell densities were then normalized to coral surface area (cells cm⁻²) (Stimson and Kinzie, 1991; Veal et al., 2010).

Chlorophyll a content

Duplicate 3 ml samples from the tissue slurry were centrifuged (3450 rpm for 3 min) (Fisher Scientific accuSpinTM 3R) to isolate the algal pellet before 5 ml of 100% acetone was added to extract

chlorophyll a at -20° C for 36 h in the dark. The supernatant of the extract was measured spectrophotometrically (λ =630, 663 and 750 nm) (Shimadzu UV-2450, Kyoto, Kyoto Prefecture, Japan) and concentrations of chlorophyll a were calculated using equations specified for dinoflagellates from Jeffrey and Humphrey (1975), after accounting for an acetone blank. The chlorophyll concentrations were then normalized to surface area (μ g cm⁻²) and to endosymbiont cells (pg cell⁻¹).

Tissue biomass

Triplicate 1 ml aliquots from each coral tissue slurry were pipetted into pre-burned (450° C for 5 h) aluminium pans in a muffle furnace (Fisher Scientific Isotemp Muffle Furnace), placed in a drying oven (Fisher Scientific Isotemp Oven) at 60° C for >24 h until they reached a constant mass, and then placed in the muffle furnace at 450° C for 4–6 h to determine ash-free dry mass. The difference between the dried (60° C) and burned (4–6 h at 450° C) masses is the total biomass of the aliquoted tissue slurry, and the tissue biomass was expressed as mg cm⁻².

Coral and endosymbiont tissue N content

To calculate coral and endosymbiont tissue N content, a 7 ml aliquoted tissue slurry containing coral host tissue and endosymbionts from each coral fragment was filtered through a 20 µm nylon net filter (Wildco®, Yulee, FL, USA) (Maier et al., 2010) to remove skeletal carbonates from each sample. The remaining host tissue and endosymbiont cells were separated by centrifugation (3450 rpm for 3 min) (Fisher Scientific accuSpinTM 3R) with 3-4 seawater rinses (Muscatine et al., 1989). Between each seawater rinse and centrifugation, microscopic inspections using a Leica Binocular Microscope (DM500, Feasterville, PA, USA) were completed to ensure separation efficiency between the coral tissue and endosymbionts. Tissues were filtered onto weighed pre-combusted 25 mm GF/F filters (Whatman®) (450°C, 4 h), dried overnight (80°C), weighed and placed in microcentrifuge tubes (Wall et al., 2018). Tissue N content for the coral hosts and algal endosymbionts were determined by the means of high-temperature (1000°C) combustion following the Dumas method (Shea and Watts, 1939) of samples in an oxygen-enriched helium atmosphere in an elemental analyzer (Control Equipment Corporation, Model CEC 440HA) at the UCSB MSI Analytical Lab. Algal endosymbiont % N content and coral tissue % N content were calculated by normalizing the N (mg) to the weight of the dry tissue mass (mg) on the filter and multiplying by 100. The N per algal endosymbiont cell (pg N cell⁻¹) was also calculated.

Holobiont metabolic response variablesEstimating saturating light levels

To determine saturating light levels for the net photosynthesis trials, we first characterized net photosynthesis as a function of PFD (commonly referred to as photosynthesis–irradiance curves) for each of the three paired sites (n=8 fragments, 4 fragments from each site). Fragments were placed in 10 identical closed-system acrylic respiration chambers (650 ml each) (Australian Institute of Marine Science, Townsville, Australia) with rotating stir bars (200 rpm), including replicate seawater-only chambers (n=2) as blanks for controls during each trial (Putnam and Gates, 2015; Silbiger et al., 2019). Individual temperature (Presens Pt1000, Regensburg, Germany) and fiber-optic oxygen probes [company two-point calibration with oxygen-free environment (nitrogen, sodium sulphite) and air-saturated environment; Presens Oxygen Dipping Probes DP-PSt7, Regensburg, Germany] were placed in each

chamber. Oxygen concentrations (μ mol l⁻¹) and temperature (°C) were recorded at a frequency of 1 Hz. Measurements were taken using a Presens Oxygen Meter [OXY-10 SMA (G2)] system with temperature correction for each individual channel. An LED light (Mars Aqua 300w LED Brand Epistar, LongGang District, ShenZhen, China) was hung above the chambers to expose the coral fragments to nine light levels to estimate net photosynthesis-PFD curves for each trial in the laboratory before experimental assays at ambient temperature (26.8°C in Mo'orea) (trial 1: 0, 29, 75, 139, 218, 350, 536, 726, 910 μ mol m⁻² s⁻¹, trial 2: 0, 61, 76, 134, 217, 347, 520, 742, 910 μ mol m⁻² s⁻¹, trial 3: 0, 65.9, 80, 141, 218, 349, 526, 716, 918 μ mol m⁻² s⁻¹). Sequential PFDs were used to identify a net photosynthesis-PFD curve fit in order to calculate saturating light (Ik) of corals prior to experimental trials. Light levels were determined by an underwater cosine corrected sensor (MQ-510 Quantum Meter, spectral range of 389–692±5 nm, Apogee Instruments, Logan, UT, USA).

Rates of oxygen evolution and consumption were determined using repeated local linear regressions with the package LoLinR (Olito et al., 2017) in R (https://www.r-project.org/), corrected for chamber volume displacement by the corals, blank seawater control rates, and normalized to coral surface area using the paraffin waxdipping technique (Stimson and Kinzie, 1991; Veal et al., 2010). LoLinR was run with the parameters of L_{pc} for linearity metric (L_{pc} =the sum of the percentile-ranks of the Z_{min} , Z scores standardized against the minimum value (Elzhov et al., 2009), for each component metric) and alpha=0.6 (minimum window size for fitting the local regressions, which is the proportion of the total observations in the data set for observations and thinning of the data from every second to every 20 s). A non-linear least squares fit (NLLS; Marshall and Biscoe, 1980) for a non-rectangular hyperbola was used to identify net photosynthesis-PFD curves (Marshall and Biscoe, 1980). The model is as follows:

$$P_{\rm net} = \frac{\varphi {\rm PAR} + \sqrt{(\varphi {\rm PPFD} + P_{\rm max})2} - 4\Theta\varphi {\rm PAR}\,P_{\rm max}}{2\Theta} - R_{\rm d}, \ (1)$$

where the parameters are $P_{\rm net}$ and $P_{\rm max}$ (area-based net and maximum gross photosynthetic rates, respectively), PPFD (photosynthetic photon flux density), $R_{\rm d}$ (dark respiration), φ (apparent quantum yield, AQY), PAR (photosynthetically active radiation) and Θ (curvature parameter, dimensionless). $I_{\rm k}$ was calculated by dividing $P_{\rm max}$ by AQY.

Based on the net photosynthesis–PFD curves, the I_k for each of the paired sites were 264.48, 367.43 and 398.47 µmol photons m⁻² s⁻¹, respectively, with no indication of photoinhibition (Fig. S1). Therefore, net photosynthetic rates were run at 563±30, 504±10 and 562 µmol m⁻² s⁻¹ for the first, second and third set of paired sites, respectively, to ensure that the experimental trials were run at saturating light conditions.

Net photosynthesis and respiration

Replicate coral fragments from each colony were assigned to light (n=48) or dark (n=48) and underwent light net photosynthesis or dark respiration heat ramping experiments. For respirometry measurements, fragments were placed in 10 individual closed-system acrylic respiration chambers (650 ml) (Australian Institute of Marine Science, Townsville, Australia) with rotating stir bars (200 rpm) to measure net photosynthesis (NP) and NC in the light, and respiration was measured in the dark. Filtered seawater (pore size \sim 100 μ m) was used for all experimental assays. Replicate seawater-only chambers were used as controls (n=2) for background normalization during each trial (n=6 light trials, n=6 dark trials) (Putnam and Gates, 2015; Silbiger et al., 2019). Each of the heat

ramping experiments began at approximately 06:30 h (dark trials were kept in complete darkness over experimental assays). Eight experimental coral fragments were moved from their ambient seawater flow-through tanks and randomly assigned to one of the 10 respirometry chambers. During each light ramp trial, the coral fragments were exposed to eight temperatures for 60 min (20, 24, 28, 30, 31, 32, 35 and 37°C) at saturating light. The dark respiration ramp trials were conducted at eight to 12 temperatures from 20 to 40° C for 20 min. Preliminary data collected in January 2019 showed no difference between $R_{\rm d}$ calculated over 60 min versus 20 min at nine different temperatures (ANOVA: $F_{3,536}$ =1.31, P=0.27; Fig. S2). Longer incubation periods were necessary in the light trials to detect a reliable difference in total alkalinity (TA) to calculate NC rates (Silbiger et al., 2019).

Temperature was controlled in an insulated reservoir using a thermostat system (Apex Controller, Neptune Systems, Morgan Hill, CA, USA) to maintain the assay temperature ($\pm 0.1^{\circ}$ C) with paired heaters (Finnex 800W Titanium Heater, Finnex 300W Titanium Heater, Burnaby, British Columbia, Canada) and chillers (Aqua Logic Delta Star®, DS-4, San Diego, CA, USA). Once the seawater in the insulated reservoir reached a stable temperature, the respirometry chambers containing both the coral fragments and controls were added and measurements started immediately. NP and $R_{\rm d}$ rates were quantified through oxygen production/consumption measured by fiber optic oxygen sensors using the same methods described above. GP was calculated as NP plus the absolute value of $R_{\rm d}$. After each incubation, we removed all coral tissue, dried the coral skeletons, and measured the surface area of each coral using the paraffin wax-dipping technique described above to normalize the rates (μ mol cm⁻² h⁻¹) (Stimson and Kinzie, 1991; Veal et al., 2010).

Net light calcification

NC was measured simultaneously during the light trials using the total alkalinity anomaly technique (Chisholm and Gattuso, 1991). Before the start of each assay temperature in the light trials, triplicate 125 ml water samples (*n*=3) were collected from the temperature-controlled seawater designated to fill the chambers to provide the starting TA value. Following the 60-min incubation period for each assay temperature, 125 ml water samples were collected from each coral (*n*=8) and blank (*n*=2) chamber. Conductivity and temperature measurements were taken for each individual water sample using a Thermo ScientificTM Orion StarTM A222 Conductivity Portable Meter and a Traceable[®] digital thermometer (Control Company 5-077-8, accuracy=0.05°C, resolution=0.001°C, Webster, TX, USA). Within 30 min of collection, the water samples were preserved with 50 μl of 50% saturated mercuric chloride (HgCl₂) in deionized water.

TA was measured using open cell potentiometric titrations following standard operating procedures (SOP 3b; Dickson et al., 2007) using an automatic titrator (Mettler-Toledo T50, Columbus, OH, USA) fitted with a InMotion Pro-sample carousel (Columbus, OH, USA). The titrator had a Mettler pH probe (DGi-115) and was operated with certified HCl titrant (batch A17, Dickson Laboratory). Certified reference material (CRM; Dickson CRM batch 180) was used to evaluate the accuracy of the TA measurements (SOP 3b; Dickson et al., 2007). A CRM was run before each sample set daily. The error was always less than 0.60% off from the certified value, and precision was <4 µEq. To calculate NC, we used Eqn 2:

$$NC = \frac{\Delta TA \times V \times \sigma}{2 \times t \times SA},$$
(2)

where ΔTA (µmol kg⁻¹) is the difference between the initial preincubation and post-incubation TA value, V (cm³) is the volume of

water in the experimental aquarium (chamber), σ (g cm⁻³) is the density of seawater, t (h) is the incubation time and SA (cm²) is the surface area of the coral samples determined by the paraffin wax-dipping technique (Stimson and Kinzie, 1991; Veal et al., 2010). Δ TA is divided by 2 because 1 mole of CaCO₃ is produced for every 2 moles of TA, and the values are expressed as μ mol cm⁻² h⁻¹. NC (μ mol cm⁻² h⁻¹) was calculated by subtracting the seawater controls to account for changes in the alkalinity anomaly due to any calcifying organisms in the seawater.

Population level response

Benthic community and P. acuta percent cover

To calculate percent cover of the benthic community and P. acuta at each site, twenty 0.5×0.5 m quadrats divided into 25 equal squares $(5 \times 5$ cm) were randomly placed (using a random number generator) along each of two 40 m transects that were laid parallel to shore starting at the coral recovery locations. The percent cover was visually estimated for P. acuta cover, total coral cover (23 genera) excluding P. acuta, total algal cover (macroalgae, turf and fleshy algae), crustose coralline algae (CCA) and substrate (bare rock, rubble, sand and/or bare space) in each quadrat with the limit of resolution being 4% change in cover. The same snorkeler measured percent cover at all six sites.

Data analysis

TPC characterization

Individual thermal performance curves for each of the biological rates of performance (μ mol cm⁻² h⁻¹) (GP, R_d and NC) (Fig. S3) were fitted to the Sharpe–Schoolfield model (see Table 1 for parameter definitions; Sharpe and Demichele, 1977; Schoolfield et al., 1981) using a non-linear least squares regression:

$$\log(\text{rate})_{i} = b(T_{c}) + E_{a} \left(\frac{1}{T_{c}} - \frac{1}{KT_{i}}\right) - \log(1 + e^{E_{h}((1/KT_{h}) - (1 - KT_{i}))}).$$
(3)

Fits were determined using the 'nls_multstart' function in the 'nls.multstart' package (https://cran.r-project.org/web/packages/minpack.lm/index.html) in R statistical software (v3.2.0) (Padfield et al., 2015). The 'nls_multstart' function allows for multiple starting values for each parameter and model selection is carried out using the Akaike information criterion (AIC) to identify the parameter set that best characterizes the data (Padfield et al., 2015). Random start parameter values are picked from a uniform distribution and the set with the lowest AIC value is retained (Padfield et al., 2015). The goodness of fit of the selected models was examined both graphically and through computation of a pseudo- R^2 value (Padfield et al., 2015). Thermal performance metrics $[T_{\rm opt}, \, \mu_{\rm max}]$ and $b(T_{\rm c})$ were then extracted from the TPC curves. $T_{\rm opt}$ and $\mu_{\rm max}]$ were calculated from the TPC parameters,

where T_{opt} is calculated as:

$$T_{\text{opt}} = \left(\frac{E_{\text{h}} \times T_{\text{h}}}{(E_{\text{h}} + (K \times T_{\text{h}} \times \log((E_{\text{h}}/E_{\text{a}}) - 1)))}\right). \tag{4}$$

 $\mu_{\rm max}$ is the rate (either GP, $R_{\rm d}$ or NC) at $T_{\rm opt}$, and $b(T_{\rm c})$ is the rate (either GP, $R_{\rm d}$ or NC) at 26.8°C (mean ambient seawater temperature conditions during the sampling period in Mo'orea).

Statistical analysis

Pearson correlation tests were used to measure the correlation between the different environmental variables [sedimentation rate $(mg cm^{-2} day^{-1}), NH_4^+ (\mu mol l^{-1}), NO_3^- + NO_2^- (\mu mol l^{-1}), PO_4^{3-}$ (μmol l⁻¹), mean temperature (°C), % tissue N, dissolved inorganic nitrogen-to-phosphorus ratios (DIN:DIP), and mean daytime PFD (μ mol photons m⁻² s⁻¹)] using the stats package in R. Because many of the environmental parameters were correlated across sites (Fig. 2), we used % tissue N (an integrated measure of nitrogen history) and sedimentation rates to represent the environmental gradient in our statistical analyses. Further, there was a significant correlation between mean temperature and % tissue N (Pearson's r=0.56, P<0.0001), and mean temperature and sedimentation (r=0.69, P<0.0001) (Fig. 2). Therefore, we used the residuals from the regression for tissue nitrogen and sedimentation against temperature as independent variables in the models, which successfully removed collinearity. Because recent thermal history influences corals' response to thermal stress (Castillo and Helmuth, 2005; Middlebrook et al., 2008; Oliver and Palumbi, 2011; Carilli et al., 2012), the residual approach allows us to test the effect of the nutrient and sedimentation environment on coral thermal tolerance metrics above and beyond the effect of background temperature (Graham, 2009; Silbiger et al., 2014).

For the endosymbiont and coral host response variables, we ran individual general linear mixed effects models for each biological parameter [chlorophyll a content ($\mu g \text{ cm}^{-2}$), endosymbiont density (×10⁶ cells cm⁻²), endosymbiont % N content, endosymbiont N content cell⁻¹ (pg N cell⁻¹), tissue biomass (mg cm⁻²) and coral tissue % N content] with % tissue N residuals (Table S1A; or sedimentation rate residuals in Table S1B) as the independent variable. For the thermal performance metrics, we ran individual models for each thermal performance metric [$T_{\rm opt}$, $\mu_{\rm max}$ and $b(T_{\rm c})$] for each specific metabolic rate process (GP, Rd and NC) with % tissue N residuals (Table S2; or sedimentation rate residuals in Table S3) as the independent variable. Site was included as a random effect in all models to account for site-level variability. We also ran a general linear model to compare the relationship between the percent cover of P. acuta colonies with % tissue N residuals (or sedimentation rate residuals, presented in Fig. S4) as the independent variable. All general linear mixed effect models were run using the lme4 package in R, and parameters were centered and standardized for all analyses. Because of the strong collinearity between nutrients and sedimentation (Pearson's r=0.83, P<0.0001;

Table 1. Parameters of the Sharpe-Schoolfield model using a non-linear least squares regression

Parameter	Units/value	Description
b(T _c)	μmol cm ⁻² h ⁻¹	Log rate of metabolism normalized to a reference temperature
E _a	eV	Activation energy
E_{h}	eV	Temperature-induced inactivation of enzyme kinetics past T_h for each population
K	$8.62 \times 10^{-5} \text{ eV K}^{-1}$	Boltzmann constant
T_{c}	299.95 K or 26.8°C	Reference temperature at which no low- or high-temperature inactivation is experienced
T_{h}	Kelvin (K)	Temperature at which half the enzymes are inactivated
T_{i}	Kelvin (K)	Temperature i

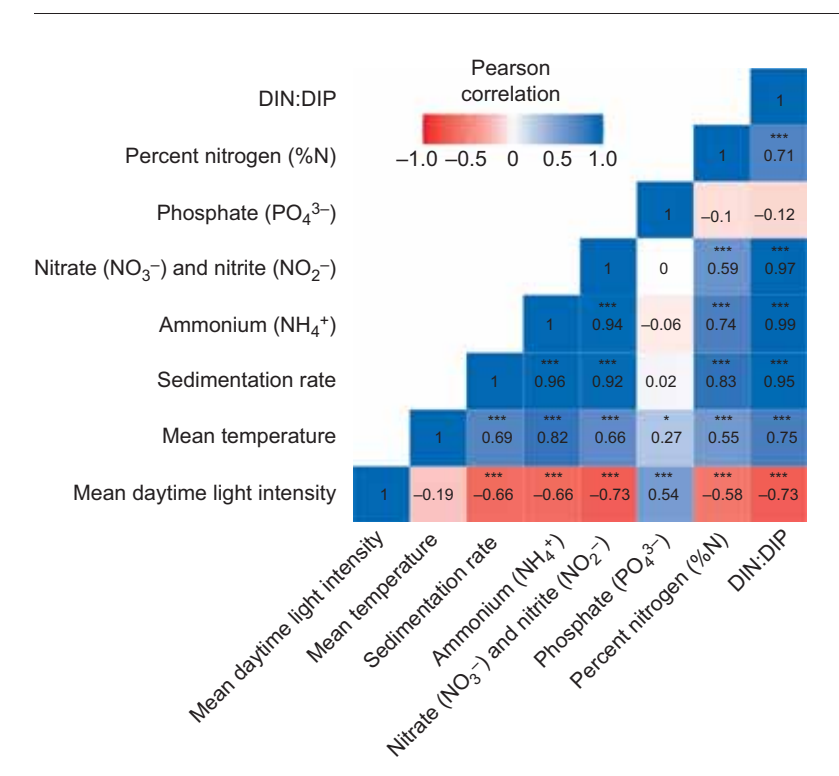


Fig. 2. Matrix of correlation coefficients for environmental data. Red background is a negative correlation, white background is low or no correlation, and blue background is a positive correlation. Significance level is shown with asterisks (**P*<0.01, ****P*<0.0001).

Fig. 2), we refer to the environmental gradient as encompassing both parameters throughout. Notably, because the nutrient and sedimentation residual models showed similar trends, we focus on the nutrient results in the main text and sedimentation results in the supplemental material (Figs S4–S6, Tables S1B, S3A–C). All data and code used for this study are available on GitHub (https://github.com/daniellembecker/Nutrient_sediment_loading_

affect_coral_functionality) and at Zenodo (https://doi.org/10.5281/zenodo.4081813).

RESULTS

Physical and chemical site characteristics

Across our six study sites, there was a gradient in nutrient concentration (% N content of *T. ornata*) and sedimentation rate, with the average % N content of *T. ornata* (n=3 per site) ranging from 0.67% to 0.89% and average sedimentation rates ranging from 1.58 to 3.44 mg cm⁻² day⁻¹. Average PO_4^{3-} , $NO_3^{-+}NO_2^{-}$, NH_4^{+} and DIN:DIP (n=2 per site) ranged from 0.34 to 0.36, 0.26 to 0.76, 0.085 to 1.49 µmol I^{-1} and 1.01 to 6.37 (Fig. 1E,F), respectively, along the north-shore fringing reef sites throughout Mo'orea (Fig. 1A). Site E had the highest average PO_4^{3-} , $NO_3^{-+}NO_2^{-}$, NH_4^{+} , DIN:DIP, % N content in *T. ornata*, and the highest sedimentation rates recorded (Fig. 1A,E,F).

Average temperature ranged from 26.5 to 27.7°C across the six sites over the 14-day logger deployment (Fig. 1C). The standard error in temperature ranged from 0.02°C to 0.04°C throughout the six sites (Fig. 1C). The average daytime PFD ranged from 1193.23 to 2677.13 μmol photons m^{-2} s $^{-1}$ across the six sites, with the lowest average daytime PFD values present at sites C, E and F, where higher sedimentation rates were recorded (Fig. 1A,D).

Endosymbiont and coral host response variables

We tested the effect of varying nutrient conditions and sedimentation rates on the chlorophyll a content (µg cm $^{-2}$), endosymbiont density (×10 6 cells cm $^{-2}$), endosymbiont % N content, endosymbiont N content cell $^{-1}$ (pg N cell $^{-1}$), tissue

biomass (mg cm $^{-2}$) and coral tissue % N content within coral fragments (Fig. 3). Average endosymbiont density and chlorophyll a content ranged from 0.75 to 1.73×10^6 cells cm $^{-2}$ and 5.03 to $10.3~\mu g$ cm $^{-2}$, respectively, with the highest densities present at site C and lowest found at site B (Fig. 1A, Table 2). Average endosymbiont % N content ranged from 14.4% to 17.4% and endosymbiont N content cell $^{-1}$ ranged from 4.06 to 5.86 pg N cell $^{-1}$. Average coral tissue biomass ranged from 6.75

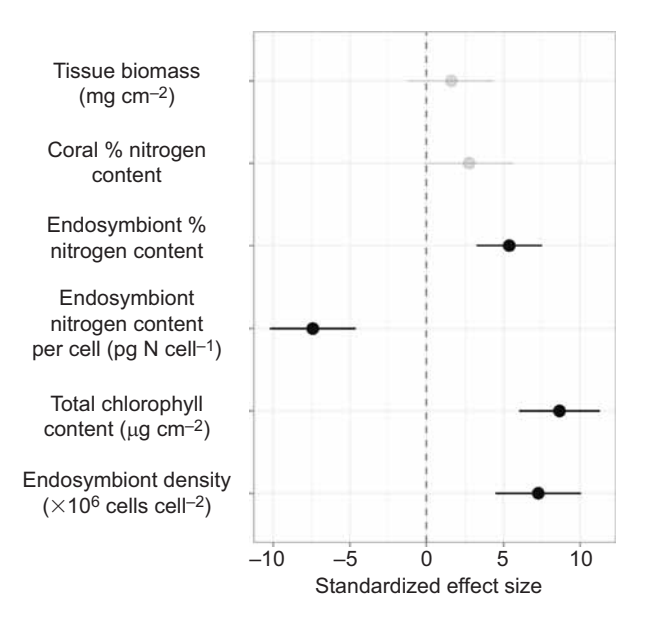


Fig. 3. Standardized effect sizes from individual mixed effects models for endosymbiont and coral host response variables as a function of % tissue N of *T. ornata* residuals (*n*=54). Values are effect sizes ±95% CI. All response variables were standardized, and values with 95% CI that do not cross zero are statistically significant (see Table S1A). The light gray/transparent variables are not statistically significant. For sedimentation results, see Fig. S5, Table S1B.

Table 2. Mean (±s.e.m.) ranges of endosymbiont, coral and holobiont metabolic response variables across all sites sites (A–F) along the nutrient and sedimentation gradient

Parameter	Site A	Site B	Site C	Site D	Site E	Site F
Endosymbiont response						
Endosymbiont % N content	15.2±0.70	17.3±1.35	17.4±2.82	17.4±1.90	14.4±2.77	17.2±1.72
Endosymbiont N content cell ⁻¹ (pg N cell ⁻¹)	5.11±0.54	5.86±0.68	4.06±0.68	5.92±1.04	4.16±1.12	5.25±0.86
Chlorophyll a content (μg cm ⁻²)	5.90±0.46	5.03±0.62	10.3±0.93	5.42±0.72	5.92±0.45	5.90±0.63
Endosymbiont density (×10 ⁶ cells cm ⁻²)	1.10±0.094	0.748±0.072	1.73±0.16	1.09±0.10	0.941±0.077	0.820±0.057
Coral response						
Tissue biomass (mg cm ⁻²)	10.5±0.71	7.70±0.73	10.1±1.15	9.39±0.96	6.75±0.33	8.13±0.64
Coral tissue % N content	22.8±1.12	18.0±1.02	20.7±1.44	24.3±2.43	19.4±1.38	24.6±1.91
Holobiont response						
T _{opt} (°C)						
Gross photosynthesis	29.9±0.12	30.0±0.23	29.6±0.22	30.7±0.22	31.0±0.53	31.2±0.57
Dark respiration	35.4±0.41	34.5±0.27	33.3±0.22	32.9±0.34	35.8±0.71	36.1±0.81
Net light calcification	29.8±0.65	28.5±0.76	29.5±0.71	30.2±0.99	29.7±0.52	30.7±1.19
μ_{max} (μ mol cm ⁻² h ⁻¹)						
Gross photosynthesis	1.00±0.056	1.18±0.022	1.03±0.050	0.89±0.043	0.81±0.037	1.05±0.044
Dark respiration	0.43±0.027	0.54±0.020	0.48±0.036	0.48±0.014	0.48±0.019	0.60±0.040
Net light calcification	0.34±0.029	0.35±0.027	0.32±0.028	0.25±0.024	0.23±0.010	0.22±0.0096
$b(T_{c})$ (µmol cm ⁻² h ⁻¹)						
Gross photosynthesis	0.97±0.057	1.12±0.031	1.01±0.054	0.83±0.045	0.77±0.049	0.96±0.053
Dark respiration	0.33±0.024	0.44±0.022	0.43±0.041	0.42±0.014	0.36±0.019	0.46±0.030
Net light calcification	0.54±0.16	0.97±0.31	0.50±0.074	0.29±0.046	0.30±0.056	0.41±0.160

to 10.5 mg cm⁻², with the highest biomass present at site A and the lowest at site E (Fig. 1A, Table 2). Average coral tissue % N content ranged from 18.0% to 24.6%, with the highest coral tissue % N content at site F and the lowest at site B (Fig. 1A, Table 2).

Parameters associated with endosymbiont physiology significantly changed as a function of nutrient and sediment loading. Endosymbiont % N content, endosymbiont density $(\times 10^6 \text{ cells cm}^{-2})$ and total chlorophyll content (µg cm⁻²) significantly increased by 5.37%, 7.27% and 8.65% per unit change along the nutrient gradient, respectively ($F_{1,139}$ =24.28, P < 0.0001; $F_{1,139} = 26.08$, P < 0.0001; $F_{1,139} = 41.55$, P < 0.0001, respectively; Fig. 3, Table S1), while endosymbiont N content cell⁻¹ (pg N cell⁻¹) significantly decreased by 7.42% per unit change along the nutrient gradient ($F_{1.130}$ =26.96, P<0.0001; Fig. 3, Table S1). Parameters associated with the coral host, coral tissue % N content and tissue biomass (mg cm⁻²) increased slightly, but non-significantly, by 2.75% and 1.59% per unit change along the nutrient gradient, respectively $(F_{1,139}=3.46, P=0.063;$ $F_{1,139}$ =1.26, P=0.26; Fig. 3, Table S1). Further, the effect of the nutrient/sedimentation gradient on endosymbiont % N content was two times greater than the effect on coral tissue % N content (Fig. 3).

Thermal performance metrics

Thermal performance metrics and holobiont metabolic responses varied across our six north-shore fringing reef study sites in Mo'orea (Fig. 1A, Table 2). Average acute $T_{\rm opt}$ for GP, $R_{\rm d}$ and NC rates varied by 1.6, 3.2 and 2.2°C, respectively, across all sites. Average $\mu_{\rm max}$ for GP, $R_{\rm d}$ and NC rates changed by 0.37, 0.17 and 0.13 μ mol cm⁻² h⁻¹, respectively, across all sites. Notably, $\mu_{\rm max}$ GP and NC rates were low or lowest at site E (Fig. 1A, Table 2), the site with highest % N content of *T. ornata*, and highest at site B, where the lowest % N content of *T. ornata* was recorded. Average $b(T_{\rm c})$ for GP, $R_{\rm d}$ and NC rates ranged by 0.35, 0.12 and 0.68 μ mol cm⁻² h⁻¹, respectively, across all sites.

We found that elevated nutrient and sediment loading generally lowered the metabolic responses of corals to acute thermal stress in terms of their thermal sensitivity and performance. Specifically, $T_{\rm opt}$ for $R_{\rm d}$ significantly decreased by 4.75% per unit change along the nutrient gradient ($F_{1.38}$ =8.68, P<0.01; Fig. 4, Table S2), while the

 $T_{\rm opt}$ values for GP and NC were unaffected along the gradient $(F_{1,45}=0.0037,\ P=0.95;\ F_{1,45}=0.12,\ P=0.73;\ Fig. 4,\ Table S2).$ Further, the $\mu_{\rm max}$ significantly decreased by 3.32% per unit change along the nutrient gradient for GP $(F_{1,45}=9.17,\ P<0.01;\ Fig. 4,\ Table S2)$ and decreased slightly by 1.07% per unit change along the nutrient gradient, but non-significantly for NC $(F_{1,45}=3.07,\ P=0.087;\ Fig. 4,\ Table S2)$. There was no effect of the environmental gradient on $\mu_{\rm max}$ for $R_{\rm d}$ $(F_{1,45}=0.29,\ P=0.59;\ Fig. 4,\ Table S2)$. GP and NC had significantly lower $b(T_{\rm c})$ values $(F_{1,45}=5.49,\ P=0.024;\ F_{1,45}=4.63,\ P=0.037;\ Fig. 4,\ Table S2)$, with a decrease in $b(T_{\rm c})$ by 2.79% and 5.19% per unit change along the nutrient gradient, respectively, but $b(T_{\rm c})$ for $R_{\rm d}$ was unaffected by nutrient loading $(F_{1,45}=0.98,\ P=0.33;\ Fig. 4,\ Table S2)$.

Percent cover

The percent cover of P. acuta colonies decreased significantly, from 16% to 0.25%, with nutrient and sedimentation loading $(F_{1,139}=143.37,\ r^2=0.51,\ P<0.0001;\ Fig. 5;\ Fig. S3)$. Total coral cover of all 23 genera observed, excluding P. acuta, ranged from 23.25% to 49.75%, with the highest coral cover at site B (Fig. 1A,B) and the lowest at site F (Fig. 1A,B). The algal community also fluctuated across the six sites, with algal cover varying from 14.5% to 37.15%, with the highest algal cover at site F (Fig. 1A,B). Further, CCA average cover ranged from 1.25% to 15.25% across sites, with the highest CCA cover at site A (Fig. 1A,B) and the lowest at site D (Fig. 1A,B).

DISCUSSION

Our study found that coral metabolic responses significantly decreased in metrics linked to thermal sensitivity and performance along a natural nutrient and sedimentation gradient, which may have contributed to a decline in *P. acuta* percent cover. To our knowledge, this is one of the first studies that provides evidence for the influence of nutrient and sediment loading on coral thermal performance that encompasses multiple aspects of coral functionality, including endosymbiont and coral host response variables, holobiont metabolic response variables and percent cover.

It is well documented that the combined effects of nutrients and sedimentation negatively impact numerous physiological processes

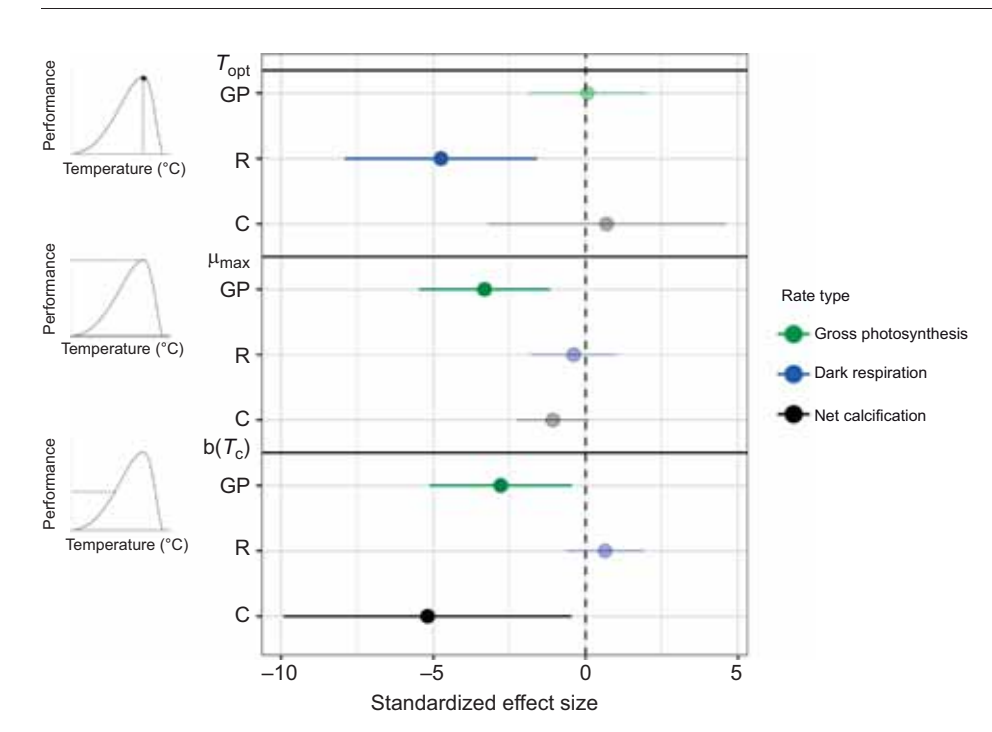


Fig. 4. Standardized effect sizes from individual mixed effects models for thermal performance metrics as a function of % tissue N *T. ornata* residuals (*n*=48). Values are effect sizes ±95% CI. 95% CI that do not cross zero are statistically significant (see Table S2). Transparent symbols are not statistically significant. For sedimentation results, see Fig. S6, Table S3.

in corals (Ezzat et al., 2015; Burkepile et al., 2019; Fisher et al., 2019; Lapointe et al., 2019). Elevated nutrient exposures in laboratory experiments can lead to a reduction in coral reproductive success, calcification rates, and skeletal density or linear extension in reef-building corals (Stambler et al., 1991; Fabricius, 2005; Dunn et al., 2012). Many negative effects of nutrient enrichment on coral physiology are linked to the subsequent growth of the algal endosymbionts, leading to chemical imbalances within the coral holobiont (Morris et al., 2019). For example, elevated levels of dissolved inorganic nitrogen and phosphorus have caused increases in algal endosymbiont densities and chlorophyll a concentrations within Stylophora pistillata colonies that coincide with declines in photosynthetic rates and efficiencies (Dubinsky et al., 1990; Stambler et al., 1991). Further, phosphate limitation associated with increasing DIN:DIP ratios inhibit DNA repair in reef-building corals during thermal

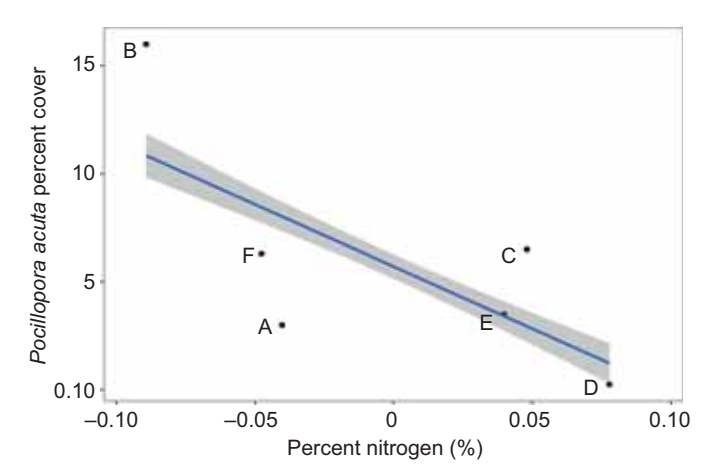


Fig. 5. Linear regression of *P. acuta* percent cover as a function of % tissue N residuals (n=6; r²=0.51, P<0.0001). Each dot is the percent cover from an individual site (A–F) along the north-shore fringing reef of Mo'orea, French Polynesia, and the blue line is the best fit line with 95% CI. For sedimentation results, see Fig. S4.

stress (Rodriguez-Casariego et al., 2018), perpetuate photodamage (Wiedenmann et al., 2013), cause competition between algal endosymbionts (Rosset et al., 2017), and potentially cause algal endosymbionts to sequester ATP from their hosts (Lin et al., 2015; Luo et al., 2017). The present study showed that DIN:DIP ratios increased along the environmental gradient, which could be a factor leading to decreased performance of corals in our experiment.

Nutrient enrichment results in an enhanced nutrient supply for the algal endosymbionts, which has been shown to increase the symbionts' use of the produced photosynthates for their own metabolic needs, at the expense of the coral host metabolism (Morris et al., 2019). Through an imbalance in nutrient delegation between the endosymbionts and coral host in the coral holobiont, competition can arise between the endosymbiont photosynthesis and host calcification for acquisition of inorganic carbon (Stambler et al., 1991; Marubini and Davies, 1996). We observed similar trends in our data regarding the increase in the endosymbiont response variables along the environmental gradient, with subsequent decreases in coral metabolism and performance. Even though the total % N content of endosymbionts increased along the environmental gradient, we saw a decrease in the pg N cell⁻¹, which indicated that competition for nitrogen likely arose between the endosymbionts owing to their population growth. In effect, the photosynthetic abilities of the endosymbiont populations within the coral fragments were depressed along the nutrient and sedimentation gradient.

Nutrient enrichment has been at the forefront of studies on local-scale stressors (e.g. Fabricius, 2005), yet suspended sediments also negatively impact corals through light attenuation (Bessell-Browne et al., 2017), reduced rates of algal endosymbiont photosynthesis (Bessell-Browne et al., 2017), and smothering of corals as a result of sediment deposition (Fabricius, 2005; Flores et al., 2012; Weber et al., 2012; Speare et al., 2019). As expected based on prior studies (Rogers, 1990; Fabricius, 2005), we saw a reduction in the mean PFD with increasing sedimentation rates throughout our sites (Figs 1A and 2), which can be detrimental to the photosynthetic abilities of the endosymbionts (Bessell-Browne et al., 2017; Cunning et al., 2017; Fisher et al., 2019). Even in nutrient-

enriched environments that show increased endosymbiont densities and/or chlorophyll a concentrations, high sediment loads can lead to a reduction in endosymbiont photosynthetic ability (Rogers, 1990; Fabricius, 2005). Although the variation in nutrient sources and DIN:DIP ratios that occur in coral reef ecosystems produces variable effects on the physiological and metabolic responses of corals (Houlbrèque and Ferrier-Pagès, 2009; Wiedenmann et al., 2013; D'Angelo and Wiedenmann, 2014; Shantz and Burkepile, 2014; Rosset et al., 2017; Lubarsky et al., 2018), increased sedimentation most often reduces coral fitness (Rogers, 1990; Fabricius, 2005; Weber et al., 2012; Fisher et al., 2019). However, few studies have shown that sediment loading could be beneficial to coral function in certain circumstances (i.e. geographic locations, reduced UV exposure or coral conspecifics) (Van Woesik et al., 2012; Bayraktarov et al., 2013; Gil, 2013; D'Angelo and Wiedenmann, 2014; Oxenford and Vallès, 2016; Morris et al., 2019), highlighting the need for a deeper understanding of coral, nutrient and sedimentation interactions.

While many studies have focused on the effects of nutrients or sediment loading on coral physiology (Rogers, 1990; Fabricius, 2005), fewer have looked at their interactions with temperature. Here, we show that nutrient and sediment loading significantly alter coral thermal responses and have strong effects on multiple aspects of coral functionality. Our results indicate that along the environmental gradient measured along the north shore of Mo'orea, $R_{\rm d}$ is less able to withstand higher temperatures, demonstrated by a decrease of 3.2°C in acute thermal optimum (T_{opt}) levels (Fig. 4). Coral populations found at sites with increased nutrients and sedimentation that experienced lower $T_{\rm opt}$ levels for $R_{\rm d}$ rates were pushed past their ability to respire at lower temperatures, which may compromise their ability to withstand increasing sea surface temperatures in the future. When respiration is depressed, the ability of corals to meet their energetic demands is hindered (Al-Horani et al., 2002; Al-Horani, 2005; Edmunds et al., 2011; Comeau et al., 2017). For example, a reduction in respiration rates can be detrimental to calcification (Al-Horani et al., 2002), photosynthesis (Rädecker et al., 2017) and reproduction (Rinkevich, 1989; Ward, 1995; Humanes et al., 2017).

In addition to generally lower thermal optima along the environmental gradient, we found that mechanisms directly linked to performance and metabolic rate processes were compromised. Specifically, the μ_{max} for GP decreased by 0.37 $\mu mol~cm^{-2}~h^{-1}$ and the $b(T_c)$ for GP and NC decreased by 0.35 and 0.68 μ mol cm⁻² h⁻¹, respectively. These results complement other studies that show that augmented nutrients and sedimentation can lead to decreased GP and NC in corals (Fabricius, 2005; Bessell-Browne et al., 2017; Morris et al., 2019). For example, a study found that elevated levels of dissolved inorganic nitrogen (13 or 5 µmol l⁻¹ increase) and inorganic nitrogen plus phosphate (13 µmol l⁻¹ nitrogen and 0.4 µmol l⁻¹ phosphate increase) led to a decrease ~ 0.08 mm day⁻¹ in the skeletal growth of *P. acuta* colonies, most likely owing to a decrease in the photosynthetic rate of the endosymbionts (Stambler et al., 1991). Further, an experiment studying the mechanism of calcification in the coral Galaxea fascicularis with Ca²⁺, pH and O₂ microsensors found that light, not energy generation, increased gross photosynthesis and prompted calcium uptake (Al-Horani et al., 2002). Decreased light availability along the sedimentation gradient could be one of the mechanisms leading to reduced rates for the holobiont metabolic processes (GP, R_d and NC) in our study. Because we collected corals from their natural conditions in situ, we acknowledge that many environmental parameters were working together to produce the results we

observed. Although we cannot infer specific mechanisms, mensurative studies are beneficial because they allow us to observe how corals that have been affected by long-term environmental conditions respond to thermal stress.

Physiological changes can result in reduced metabolic function within individual organisms, compromising key processes that facilitate successful reproduction and growth, ultimately influencing population dynamics. Extensive reviews have summarized how eutrophication and sedimentation reduce coral cover, diversity, richness and recruitment (e.g. Rogers, 1990; Fabricius, 2005). Generally, reefs with eutrophic conditions and high sedimentation rates tend to have lower biodiversity, recruitment and coral cover relative to sites with more oligotrophic conditions. We saw that the sites in Mo'orea with the highest levels of nutrient and sedimentation rates had the corals that were the least heat tolerant and had the lowest percent cover of *P. acuta* colonies. Our findings illustrate that nutrient and sediment loading may have negative implications for coral thermal performance and ecological function.

Acute TPCs in the context of our experiment are sometimes referred to as instantaneous thermal 'stress tests' because the short acclimation times do not take into account the absolute acclimation potential of the organism (Angilletta, 2009; Schulte et al., 2011). Further, the absolute values for acute thermal optima are higher than would be expected for longer-term thermal stress (Silbiger et al., 2019). However, as long as important assumptions and experimental frameworks are addressed (Schulte et al., 2011; Sinclair et al., 2016), acute TPC measurements are valuable for comparative analyses for ectothermic organisms that describe constraints on thermal acclimation (Schulte et al., 2011; Rohr et al., 2018; Voolstra et al., 2020). TPCs are unique as they allow us to observe variation between organisms through multiple metrics. Populations can span broad geographic ranges from latitudinal to altitudinal gradients, experiencing variable thermal environments (Angilletta, 2009). Therefore, some organisms may be plastic in their thermal performance. For example, when a population of Porites cylindrica coral colonies was exposed to an acute temperature ramp of 5°C above or below the local average temperature, the TPCs of the colonies shifted vertically (change in μ_{max}) and horizontally (change in T_{opt}), but there was no change to their performance breadth (Jurriaans and Hoogenboom, 2019). Further, TPCs allow us to uncover mechanistic relationships that may elicit variable metabolic responses dependent on where the relationships fall along a TPC, which are not possible using an ANOVA-style design with only a few temperature treatments (Edmunds et al., 2011; Johnson et al., 2017; Serrano et al., 2018; Wall et al., 2018).

There have been numerous studies across taxa ranging from microbes to macrofauna that use a TPC approach, which have provided valuable metrics to compare thermal tolerance across geographic ranges, populations, organisms and species (Angilletta et al., 2004; Dell et al., 2013). The TPC approach is also a useful tool to understand how organisms have responded in the past and how they may fare in future climatic conditions (Huey and Kingsolver, 1993; Angilletta, 2009). Notably, there are relatively few TPC studies of coral reef organisms (but see Rodolfo-Metalpa et al., 2014; Aichelman et al., 2019; Jurriaans and Hoogenboom, 2019; Silbiger et al., 2019; Voolstra et al., 2020). To our knowledge, this is the first study to identify how nutrient and sediment loading influence coral thermal tolerance in an explicit TPC context. Understanding how thermal tolerance is impacted by local-scale stressors can provide insight into the metabolic responses of various

organisms and how this may scale to affect larger ecosystem function. Because we saw depressed coral metabolic responses along a nutrient and sedimentation gradient, it would be beneficial to use this approach to examine the interactive effect of other anthropogenic stressors on the thermal tolerance of many species across habitats and varying geographic locations.

The results from this study demonstrate that the metabolic processes in corals, which are present in many other invertebrate species, required for growth, survival and thermal performance were negatively affected by a natural nutrient and sedimentation gradient along a coastal coral reef ecosystem. Further, the reduction in metabolic function along the environmental gradient could compromise benthic community cover throughout our sites. These results indicate that anthropogenic stressors on a local scale may further impede coral functions (e.g. photosynthesis, respiration and calcification), which could have dire consequences in their response to global anthropogenic stressors. Our findings also provide valuable information for the use of thermal performance curves to further understand how organisms across environments may respond to local- and global-scale anthropogenic stressors in concert.

Acknowledgements

We thank the Mo'orea Coral Reef Long-term Ecological Research Network, the University of California, Berkeley, Richard B. Gump South Pacific Research Station, the University of California, Santa Barbara, Marine Science Institutes Analytical Lab, and California State University, Northridge (CSUN), for facilities support. Special thanks to D. Barnas for her support and dedication in collecting data in the field. Additionally, thanks to Dr P. J. Edmunds and Dr R. C. Carpenter for their guidance and support, and Dr C. B. Wall, K. H. Wong, Dr H. M. Putnam and H. G. Reich for their valuable methodological advice for endosymbiont and coral host response variable processing. This work represents a contribution of the Mo'orea Coral Reef (MCR) LTER Site and is CSUN Marine Biology contribution number 312.

Competing interests

The authors declare no competing or financial interests.

Author contributions

Conceptualization: D.M.B., N.J.S.; Methodology: D.M.B., N.J.S.; Software: D.M.B., N.J.S.; Validation: D.M.B., N.J.S.; Formal analysis: D.M.B., N.J.S.; Investigation: D.M.B., N.J.S.; Resources: D.M.B., N.J.S.; Data curation: D.M.B., N.J.S.; Writing original draft: D.M.B., N.J.S.; Writing - review & editing: D.M.B., N.J.S.; Visualization: D.M.B., N.J.S.; Supervision: D.M.B., N.J.S.; Project administration: D.M.B., N.J.S.; Funding acquisition: D.M.B., N.J.S.

Funding

This research was funded in part by California State University, Northridge (CSUN) to N.J.S., U. S. National Science Foundation OCE#19-24281 to N.J.S., the American Academy of Underwater Sciences Foundations 2018 Masters Research Scholarship to D.M.B., CSUN Office of Graduate Studies, Department of Biology, Associated Students, College of Sciences and Mathematics, and Research and Graduate Studies to D.M.B., and the National Science Foundation Graduate Research Fellowship to DMB. Materials are in this study based upon work supported by the U. S. National Science Foundation under grant OCE#16-37396 as well as a generous gift from the Gordon and Betty Moore Foundation.

Data availability

All R code and data are available on GitHub at https://github.com/daniellembecker/ Nutrient_sediment_loading_affect_coral_functionality and at Zenodo (https://doi.org/10.5281/zenodo.4081813).

Supplementary information

Supplementary information available online at https://jeb.biologists.org/lookup/doi/10.1242/jeb.225045.supplemental

References

- Aichelman, H. E., Zimmerman, R. C. and Barshis, D. J. (2019). Adaptive signatures in thermal performance of the temperate coral Astrangia poculata. J. Exp. Biol. 222, jeb.189225. doi:10.1242/jeb.189225
- Al-Horani, F. A. (2005). Effects of changing seawater temperature on photosynthesis and calcification in the scleractinian coral Galaxea fascicularis,

- measured with O_2 , Ca^{2+} and pH microsensors. *Sci. Mar.* **69**, 347-354. doi:10. 3989/scimar 2005 69n3347
- Al-Horani, F. A., Al-Moghrabi, S. M. and De Beer, D. (2002). The mechanism of calcification and its relation to photosynthesis and respiration in the scleractinian coral *Galaxea fascicularis*. *Mar. Biol.* 142, 419-426. doi:10.1007/s00227-002-0981-8
- Andrews, R. M. and Schwarzkopf, L. (2012). Thermal performance of squamate embryos with respect to climate, adult life history, and phylogeny. *Biol. J. Linn.* Soc. 106, 851-864. doi:10.1111/j.1095-8312.2012.01901.x
- Angilletta, M. J., Jr. (2009). Thermal Adaptation: A Theoretical and Empirical Synthesis. Oxford University Press.
- Angilletta, M. J., Steury, T. D. and Sears, M. W. (2004). Temperature, growth rate, and body size in ectotherms: fitting pieces of a life-history puzzle. *Integr. Comp. Biol.* 44, 498-509. doi:10.1093/icb/44.6.498
- Bahr, K. D., Rodgers, K. S. and Jokiel, P. L. (2018). Ocean warming drives decline in coral metabolism while acidification highlights species-specific responses. *Mar. Biol. Res.* 14, 924-935. doi:10.1080/17451000.2018.1551616
- Baumann, J. H., Ries, J. B., Rippe, J. P., Courtney, T. A., Aichelman, H. E., Westfield, I. and Castillo, K. D. (2019). Nearshore coral growth declining on the Mesoamerican Barrier Reef System. *Glob. Chang. Biol.* 25, 3932-3945. doi:10. 1111/qcb.14784
- Bayraktarov, E., Pizarro, V., Eidens, C., Wilke, T. and Wild, C. (2013). Bleaching susceptibility and recovery of Colombian Caribbean corals in response to water current exposure and seasonal upwelling. PLoS ONE 8, e80536. doi:10.1371/journal.pone.0080536
- Bellwood, D. R. and Hughes, T. P. (2001). Regional-scale assembly rules and biodiversity of coral reefs. *Science* **292**, 1532-1535. doi:10.1126/science. 1058635
- Bessell-Browne, P., Negri, A. P., Fisher, R., Clode, P. L. and Jones, R. (2017). Impacts of light limitation on corals and crustose coralline algae. *Sci. Rep.* **7**, 11553. doi:10.1038/s41598-016-0028-x
- Bestion, E., Schaum, C.-E. and Yvon-Durocher, G. (2018). Nutrient limitation constrains thermal tolerance in freshwater phytoplankton. *Limnol. Oceanogr. Lett.* 3, 436-443. doi:10.1002/lol2.10096
- Bongiorni, L., Shafir, S., Angel, D. and Rinkevich, B. (2003). Survival, growth and gonad development of two hermatypic corals subjected to in situ fish-farm nutrient enrichment. *Mar. Ecol. Prog. Ser.* **253**, 137-144. doi:10.3354/meps253137
- Bruno, J. F. and Selig, E. R. (2007). Regional decline of coral cover in the Indo-Pacific: timing, extent, and subregional comparisons. *PLoS ONE* **2**, e711. doi:10. 1371/journal.pone.0000711
- Bruno, J. F., Selig, E. R., Casey, K. S., Page, C. A., Willis, B. L., Harvell, C. D., Sweatman, H. and Melendy, A. M. (2007). Thermal stress and coral cover as drivers of coral disease outbreaks. *PLoS Biol.* 5, e124. doi:10.1371/journal.pbio. 0050124
- Burke, L., Reytar, K., Spalding, M. and Perry, A. (2011). Reefs at Risk Revisited. World Resources Institute.
- Burkepile, D. E. and Hay, M. E. (2006). Herbivore vs. nutrient control of marine primary producers: context-dependent effects. *Ecology.* 87, 3128-3139. doi:10. 1890/0012-9658(2006)87[3128:HVNCOM]2.0.CO;2
- Burkepile, D. E., Shantz, A. A., Adam, T. C., Munsterman, K. S., Speare, K. E., Ladd, M. C., Rice, M. M., Ezzat, L., McIlroy, S., Wong, J. C. Y. et al. (2019). Nitrogen identity drives differential impacts of nutrients on coral bleaching and mortality. *Ecosystems* 23, 798-811. doi:10.1007/s10021-019-00433-2
- Carilli, J. E., Norris, R. D., Black, B. A., Walsh, S. M. and McField, M. (2009). Local stressors reduce coral resilience to bleaching. *PLoS ONE* 4, e6324. doi:10. 1371/journal.pone.0006324
- Carilli, J., Donner, S. D. and Hartmann, A. C. (2012). Historical temperature variability affects coral response to heat stress. *PLoS ONE* 7, 1-9. doi:10.1371/journal.pone.0034418
- Carpenter, R. (2019). Moorea Coral Reef LTER: Coral Reef: Benthic Photosynthetically Active Radiation (PAR) Data, ongoing since 2009. knb-ltermcr.4005.10. doi:10.6073/pasta/b5a2cf517337e302514fa22e172a23a0
- Castillo, K. D. and Helmuth, B. S. T. (2005). Influence of thermal history on the response of Montastraea annularis to short-term temperature exposure. Mar. Biol. 148, 261-270. doi:10.1007/s00227-005-0046-x
- Chisholm, J. R. M. and Gattuso, J.-P. (1991). Validation of the alkalinity anomaly technique for investigating calcification of photosynthesis in coral reef communities. *Limnol. Oceanogr.* 36, 1232-1239. doi:10.4319/lo.1991.36.6.1232
- Comeau, S., Carpenter, R. C. and Edmunds, P. J. (2017). Effects of pCO₂ on photosynthesis and respiration of tropical scleractinian corals and calcified algae. *ICES J. Mar. Sci.* 74, 1092-1102. doi:10.1093/icesjms/fsv267
- Courtial, L., Bielsa, V. P., Houlbrèque, F. and Ferrier-Pagès, C. (2018). Effects of ultraviolet radiation and nutrient level on the physiological response and organic matter release of the scleractinian coral *Pocillopora damicornis* following thermal stress. *PLoS ONE* 13, e0205261. doi:10.1371/journal.pone.0205261
- Cowburn, B., Samoilys, M. A. and Obura, D. (2018). The current status of coral reefs and their vulnerability to climate change and multiple human stresses in the Comoros Archipelago, Western Indian Ocean. *Mar. Pollut. Bull.* 133, 956-969. doi:10.1016/j.marpolbul.2018.04.065

- Cunning, R. and Baker, A. C. (2013). Excess algal symbionts increase the susceptibility of reef corals to bleaching. *Nat. Clim. Chang.* 3, 259-262. doi:10. 1038/nclimate1711
- Cunning, R., Muller, E. B., Gates, R. D. and Nisbet, R. M. (2017). A dynamic bioenergetic model for coral-Symbiodinium symbioses and coral bleaching as an alternate stable state. J. Theor. Biol. 431, 49-62. doi:10.1016/j.jtbi.2017.08.003
- D'Angelo, C. and Wiedenmann, J. (2014). Impacts of nutrient enrichment on coral reefs: new perspectives and implications for coastal management and reef survival. Curr. Opin. Environ. Sustain. 7, 82-93. doi:10.1016/j.cosust.2013.11.029
- Darling, E. S., Alvarez-Filip, L., Oliver, T. A., Mcclanahan, T. R. and Côté, I. M. (2012). Evaluating life-history strategies of reef corals from species traits. *Ecol. Lett.* 15, 1378-1386. doi:10.1111/j.1461-0248.2012.01861.x
- Darling, E. S., McClanahan, T. R. and Côté, I. M. (2013). Life histories predict coral community disassembly under multiple stressors. Glob. Chang. Biol. 19, 1930-1940. doi:10.1111/gcb.12191
- De'ath, G., Lough, J. M. and Fabricius, K. E. (2009). Declining coral calcification on the Great Barrier Reef. Science 323, 116-119. doi:10.1126/science.1165283
- De'ath, G., Fabricius, K. E., Sweatman, H. and Puotinen, M. (2012). The 27-year decline of coral cover on the Great Barrier Reef and its causes. *Proc. Natl. Acad.* Sci. USA 109, 17995-17999. doi:10.1073/pnas.1208909109
- DeCarlo, T. M., Cohen, A. L., Wong, G. T. F., Shiah, F.-K., Lentz, S. J., Davis, K. A., Shamberger, K. E. F. and Lohmann, P. (2017). Community production modulates coral reef pH and the sensitivity of ecosystem calcification to ocean acidification. J. Geophys. Res. Ocean. 122, 745-761. doi:10.1002/2016JC012326
- Dell, A. I., Pawar, S. and Savage, V. M. (2011). Systematic variation in the temperature dependence of physiological and ecological traits. *Proc. Natl. Acad.* Sci. USA 108, 10591-10596. doi:10.1073/pnas.1015178108
- Dell, A. I., Pawar, S. and Savage, V. M. (2013). The thermal dependence of biological traits. *Ecology* 94, 1205-1206. doi:10.1890/12-2060.1
- Dickson, A. G., Sabine, C. L. and Christian, J. R. (2007). Guide to Best Practices for Ocean CO₂ Measurements. North Pacific Marine Science Organization.
- Donovan, M. K., Adam, T. C., Shantz, A. A., Speare, K. E., Munsterman, K. S., Rice, M. M., Schmitt, R. J., Holbrook, S. J. and Burkepile, D. E. (2020). Nitrogen pollution interacts with heat stress to increase coral bleaching across the seascape. *Proc. Natl. Acad. Sci. USA* 117, 5351-5357. doi:10.1073/pnas. 1915395117
- Dubinsky, Z., Stambler, N., Ben Zion, M., McCloskey, L. R., Muscatine, L. and Falkowski, P. G. (1990). The effect of external nutrient resources on the optical properties and photosynthetic efficiency of *Stylophora pistillata*. *Proc. R. Soc. London. Ser. B* 239, 231-246. doi:10.1098/rspb.1990.0015
- Dunn, J. G., Sammarco, P. W. and LaFleur, G. (2012). Effects of phosphate on growth and skeletal density in the scleractinian coral *Acropora muricata*: a controlled experimental approach. *J. Exp. Mar. Bio. Ecol.* 411, 34-44. doi:10.1016/ i.iembe.2011.10.013
- Edmunds, P. J., Cumbo, V. and Fan, T.-Y. (2011). Effects of temperature on the respiration of brooded larvae from tropical reef corals. *J. Exp. Biol.* **214**, 2783-2790. doi:10.1242/jeb.055343
- Ezzat, L., Maguer, J.-F., Grover, R. and Ferrier-Pagés, C. (2015). New insights into carbon acquisition and exchanges within the coral–dinoflagellate symbiosis under NH₄⁺ and NO₃⁻ supply. *Proc. R. Soc. B Biol. Sci.* **282**, 20150610. doi:10. 1098/rspb.2015.0610
- Fabricius, K. E. (2005). Effects of terrestrial runoff on the ecology of corals and coral reefs: review and synthesis. *Mar. Pollut. Bull.* 50, 125-146. doi:10.1016/j. marpolbul.2004.11.028
- Faxneld, S., Jörgensen, T. L. and Tedengren, M. (2010). Effects of elevated water temperature, reduced salinity and nutrient enrichment on the metabolism of the coral *Turbinaria mesenterina*. Estuar. Coast. Shelf. Sci. 88, 482-487. doi:10.1016/ i.ecss.2010.05.008
- Fisher, R., Bessell-Browne, P. and Jones, R. (2019). Synergistic and antagonistic impacts of suspended sediments and thermal stress on corals. *Nat. Commun.* 10, 1-9. doi:10.1038/s41467-019-10288-9
- Flores, F., Hoogenboom, M. O., Smith, L. D., Cooper, T. F., Abrego, D. and Negri, A. P. (2012). Chronic exposure of corals to fine sediments: lethal and sublethal impacts. *PLoS ONE* **7**, e37795. doi:10.1371/journal.pone.0037795
- Fong, P., Donohoe, R. M. and Zedler, J. B. (1994). Nutrient concentration in tissue of the macroalga *Enteromorpha* as a function of nutrient history: an experimental evaluation using field microcosms. *Mar. Ecol. Prog. Ser.* **106**, 273-281. doi:10. 3354/meps106273
- Fong, J., Lim, Z. W., Bauman, A. G., Valiyaveettil, S., Liao, L. M., Yip, Z. T. and Todd, P. A. (2019). Allelopathic effects of macroalgae on *Pocillopora acuta* coral larvae. *Mar. Environ. Res.* **151**, 104745. doi:10.1016/j.marenvres.2019.06.007
- Gibbin, E. M., Putnam, H. M., Gates, R. D., Nitschke, M. R. and Davy, S. K. (2014). Species-specific differences in thermal tolerance may define susceptibility to intracellular acidosis in reef corals. *Mar. Biol.* 162, 717-723. doi:10.1007/ s00227-015-2617-9
- Gil, M. A. (2013). Unity through nonlinearity: a unimodal coral-nutrient interaction. Ecology 94, 1871-1877. doi:10.1890/12-1697.1
- **Graham, M. H.** (2009). Confronting multicollinearity in ecological multiple regression. *Ecology* **84**, 2809-2815. doi:10.1890/02-3114

- Hadjioannou, L., Jimenez, C., Rottier, C., Sfenthourakis, S. and Ferrier-pagès, C. (2019). Response of the temperate scleractinian coral *Cladocora caespitosa* to high temperature and long-term nutrient enrichment. *Sci. Rep.* 9, 1-11. doi:10. 1038/s41598-019-50716-w
- Halpern, B. S., Walbridge, S., Selkoe, K. A., Kappel, C. V., Micheli, F., D'Agrosa, C., Bruno, J. F., Casey, K. S., Ebert, C., Fox, H. E. et al. (2008). A global map of human impact on marine ecosystems. *Science* 319, 948-952. doi:10.1126/science.1149345
- Harvell, C. D., Mitchell, C. E., Ward, J. R., Altizer, S., Dobson, A. P., Ostfeld, R. S. and Samuel, M. D. (2002). Climate warming and disease risks for terrestrial and marine biota. Science 296, 2158-2162. doi:10.1126/science.1063699
- Hobday, A. J., Alexander, L. V., Perkins, S. E., Smale, D. A., Straub, S. C., Oliver, E. C. J., Benthuysen, J. A., Burrows, M. T., Donat, M. G., Feng, M. et al. (2016). A hierarchical approach to defining marine heatwaves. *Prog. Oceanogr.* 141, 227-238. doi:10.1016/j.pocean.2015.12.014
- Hoegh-Guldberg, O., Mumby, P. J., Hooten, A. J., Steneck, R. S., Greenfield, P., Gomez, E., Harvell, C. D., Sale, P. F., Edwards, A. J., Caldeira, K. et al. (2007). Coral reefs under rapid climate change and ocean acidification. *Science* 318, 1737-1742. doi:10.1126/science.1152509
- Hoegh-Guldberg, O., Poloczanska, E. S., Skirving, W. and Dove, S. (2017). Coral reef ecosystems under climate change and ocean acidification. *Front. Mar. Sci.* 4, 158. doi:10.3389/fmars.2017.00158
- Houlbrèque, F. and Ferrier-Pagès, C. (2009). Heterotrophy in tropical scleractinian corals. *Biol. Rev.* **84**. 1-17. doi:10.1111/i.1469-185X.2008.00058.x
- Huey, R. B. and Kingsolver, J. G. (1989). Evolution of thermal sensitivity of ectotherm performance. *Trends. Ecol. Evol.* 4, 131-135. doi:10.1016/0169-5347(89)90211-5
- Huey, R. B. and Kingsolver, J. G. (1993). Evolution of resistance to high temperature in ectotherms. Am. Nat. 142, S21-S46. doi:10.1086/285521
- Huey, R. B. and Stevenson, R. D. (1979). Integrating thermal physiology and ecology of ectotherms: a discussion of approaches. *Am. Zool.* 19, 357-366. doi:10.1093/icb/19.1.357
- Hughes, T. P., Rodrigues, M. J., Bellwood, D. R., Ceccarelli, D., Hoegh-Guldberg, O., McCook, L., Moltschaniwskyj, N., Pratchett, M. S., Steneck, R. S. and Willis, B. (2007). Phase shifts, herbivory, and the resilience of coral reefs to climate change. Curr. Biol. 17, 360-365. doi:10.1016/j.cub.2006.12.049
- Hughes, T. P., Barnes, M. L., Bellwood, D. R., Cinner, J. E., Cumming, G. S., Jackson, J. B. C., Kleypas, J., van de Leemput, I. A., Lough, J. M., Morrison, T. H. et al. (2017). Coral reefs in the Anthropocene. *Nature* 546, 82-90. doi:10.1038/nature22901
- Hughes, T. P., Anderson, K. D., Connolly, S. R., Heron, S. F., Kerry, J. T., Lough, J. M., Baird, A. H., Baum, J. K., Berumen, M. L., Bridge, T. C. et al. (2018). Spatial and temporal patterns of mass bleaching of corals in the Anthropocene. *Science* 359, 80-83, doi:10.1126/science.aan8048
- Humanes, A., Ricardo, G. F., Willis, B. L., Fabricius, K. E. and Negri, A. P. (2017). Cumulative effects of suspended sediments, organic nutrients and temperature stress on early life history stages of the coral *Acropora tenuis*. Sci. Rep. 7, 44101. doi:10.1038/srep44101
- Jeffrey, S.T. and Humphrey, G.F. (1975). New spectrophotometric equations for determining chlorophylls a, b, c1 and c2 in higher plants, algae and natural phytoplankton. *Biochem. Physiol. Pflanzen* 167, 191-194.
- Johnson, K. S., Petty, R. L. and Thomsen, J. (1985). Flow-injection analysis for seawater micronutrients. In *Mapping Strategies in Chemical Oceanography* (ed. A. Zirino), pp. 7-30. American Chemical Society.
- Johnson, M. D., Comeau, S., Lantz, C. A. and Smith, J. E. (2017). Complex and interactive effects of ocean acidification and temperature on epilithic and endolithic coral-reef turf algal assemblages. *Coral Reefs.* 36, 1059-1070. doi:10.1007/s00338-017-1597-2
- Jurriaans, S. and Hoogenboom, M. O. (2019). Thermal performance of scleractinian corals along a latitudinal gradient on the Great Barrier Reef. Philos. Trans. R. Soc. B Biol. Sci. 374, 20180546. doi:10.1098/rstb.2018.0546
- Kellermann, V., Chown, S. L., Schou, M. F., Aitkenhead, I., Janion-Scheepers, C., Clemson, A., Scott, M. T. and Sgrò, C. M. (2019). Comparing thermal performance curves across traits: how consistent are they? *J. Exp. Biol.* 222, jeb193433. doi:10.1242/jeb.193433
- Kitchen, R. M., Piscetta, M., Rocha de Souza, M., Lenz, E. A., Schar, D. W. H., Gates, R. D. and Wall, C. B. (2020). Symbiont transmission and reproductive mode influence responses of three Hawaiian coral larvae to elevated temperature and nutrients. *Coral Reefs* 39, 419-431. doi:10.1007/s00338-020-01905-x
- Koop, K., Booth, D., Broadbent, A., Brodie, J., Bucher, D., Capone, D., Coll, J., Dennison, W., Erdmann, M., Harrison, P. et al. (2001). ENCORE: The effect of nutrient enrichment on coral reefs. Synthesis of results and conclusions. *Mar. Pollut. Bull.* 42, 91-120. doi:10.1016/S0025-326X(00)00181-8
- Lapointe, B. E., Brewton, R. A., Herren, L. W., Porter, J. W. and Hu, C. (2019). Nitrogen enrichment, altered stoichiometry, and coral reef decline at Looe Key, Florida Keys, USA: a 3-decade study. *Mar. Bio.* 166, 108. doi:10.1007/s00227-019-3538-9
- Latimer, C. A. L., Wilson, R. S. and Chenoweth, S. F. (2011). Quantitative genetic variation for thermal performance curves within and among natural populations of

- Drosophila serrata. J. Evol. Biol. **24**, 965-975. doi:10.1111/j.1420-9101.2011.
- Leggat, W. P., Camp, E. F., Suggett, D. J., Heron, S. F., Fordyce, A. J., Gardner, S., Deakin, L., Turner, M., Beeching, L. J., Kuzhiumparambil, U. et al. (2019). Rapid coral decay is associated with marine heatwave mortality events on reefs. Curr. Biol. 29, 2723-2730. doi:10.1016/j.cub.2019.06.077
- **Lin, D. T. and Fong, P.** (2008). Macroalgal bioindicators (growth, tissue N, δ^{15} N) detect nutrient enrichment from shrimp farm effluent entering Opunohu Bay, Moorea, French Polynesia. *Mar. Pollut. Bull.* **56**, 245-249. doi:10.1016/j. marpolbul.2007.09.031
- Lin, S., Cheng, S., Song, B., Zhong, X., Lin, X., Li, W., Li, L., Zhang, Y., Zhang, H., Ji, Z. et al. (2015). The Symbiodinium kawagutii genome illuminates dinoflagellate gene expression and coral symbiosis. Science. 350, 691-694. doi:10.1126/science.aad0408
- Littler, M. M. and Littler, D. S. (1984). Models of tropical reef biogenesis: the contribution of algae. Prog. Phycol. Res. 3, 323-364.
- Long, M. H., Rheuban, J. E., Berg, P. and Zieman, J. C. (2012). A comparison and correction of light intensity loggers to photosynthetically active radiation sensors. *Limnol. Oceanogr. Methods* 10, 416-424. doi:10.4319/lom.2012.10.416
- Lozano-Cortés, D. F., Giraldo, A. and Izquierdo, V. (2014). Short-term assessment of the sediment deposition rate and water conditions during a rainy season on La Azufrada coral reef, Gorgona Island, Colombia. *Rev. Biol. Trop.* 62, 107-116. doi:10.15517/rbt.v62i0.15981
- Lubarsky, K. A., Silbiger, N. J. and Donahue, M. J. (2018). Effects of submarine groundwater discharge on coral accretion and bioerosion on two shallow reef flats. *Limnol. Oceanogr.* **63**, 1660-1676. doi:10.1002/lno.10799
- Luo, H., Lin, X., Li, L., Lin, L., Zhang, C. and Lin, S. (2017). Transcriptomic and physiological analyses of the dinoflagellate *Karenia mikimotoi* reveal non-alkaline phosphatase-based molecular machinery of ATP utilisation. *Environ. Microbiol.* 19, 4506-4518. doi:10.1111/1462-2920.13899
- Maier, C., Weinbauer, M. G. and Pätzold, J. (2010). Stable isotopes reveal limitations in C and N assimilation in the caribbean reef corals *Madracis auretenra*, *M. carmabi* and *M. formosa. Mar. Ecol. Prog. Ser.* 412, 103-112. doi:10.3354/ meps08674
- Marshall, B. and Biscoe, P. V. (1980). A model for C₃ leaves describing the dependence of net photosynthesis on irradiance. *Jor. Exper. Bot.* 31, 29-39. doi:10.1093/jxb/31.1.29
- Marubini, F. and Davies, P. S. (1996). Nitrate increases zooxanthellae population density and reduces skeletogenesis in corals. *Mar. Biol.* 127, 319-328. doi:10. 1007/BF00942117
- McClanahan, T. R., Sala, E., Stickels, P. A., Cokos, B. A., Baker, A. C., Starger, C. J. and Jones, S. H. (2003). Interaction between nutrients and herbivory in controlling algal communities and coral condition on Glover's Reef, Belize. *Mar. Ecol. Prog. Ser.* 261, 135-147. doi:10.3354/meps261135
- McCulloch, M. T., D'Olivo, J. P., Falter, J., Holcomb, M. and Trotter, J. A. (2017).
 Coral calcification in a changing world and the interactive dynamics of pH and DIC upregulation. *Nat. Commun.* 8, 15686. doi:10.1038/ncomms15686
- Middlebrook, R., Hoegh-Guldberg, O. and Leggat, W. (2008). The effect of thermal history on the susceptibility of reef-building corals to thermal stress. J. Exp. Biol. 211, 1050-1056. doi:10.1242/jeb.013284
- Morris, L. A., Voolstra, C. R., Quigley, K. M., Bourne, D. G. and Bay, L. K. (2019).
 Nutrient availability and metabolism affect the stability of coral—Symbiodiniaceae symbioses. *Trends Microbiol.* 27, 678-689. doi:10.1016/j.tim.2019.03.004
- Muller-Parker, G., D'elia, C. F. and Cook, C. B. (2015). Interactions between corals and their symbiotic algae. In *Coral Refs in the Anthropocene* (ed. C. Birkeland), pp. 99-116. Dordrecht: Springer.
- Muscatine, L., Falkowski, P. G., Dubinsky, Z., Cook, P. A. and McCloskey, L. R. (1989). The effect of external nutrient resources on the population dynamics of zooxanthellae in a reef coral. *Proc. R. Soc. London* 236, 311-324. doi:10.1098/ rspb.1989.0025
- Olito, C., White, C. R., Marshall, D. J. and Barneche, D. R. (2017). Estimating monotonic rates from biological data using local linear regression. J. Exp. Biol. 220, 759-764. doi:10.1242/jeb.148775
- Oliver, T. A. and Palumbi, S. R. (2011). Do fluctuating temperature environments elevate coral thermal tolerance? *Coral Reefs* **30**, 429-440. doi:10.1007/s00338-011-0721-y
- Oxenford, H. A. and Vallès, H. (2016). Transient turbid water mass reduces temperature-induced coral bleaching and mortality in Barbados. *PeerJ.* **4**, e2118. doi:10.7717/peerj.2118
- Padfield, D., Yvon-Durocher, G., Buckling, A., Jennings, S. and Yvon-Durocher, G. (2015). Rapid evolution of metabolic traits explains thermal adaptation in phytoplankton. *Ecol. Lett.* 19, 133-142. doi:10.1111/ele.12545
- Pinzón, C. J. H., Dornberger, L., Beach-Letendre, J., Weil, E. and Mydlarz, L. D. (2014). The link between immunity and life history traits in scleractinian corals. *PeerJ.* 2, e628. doi:10.7717/peerj.628
- Poquita-Du, R. C., Ng, C. S. L., Loo, J. B., Afiq-Rosli, L., Tay, Y. C., Todd, P. A., Chou, L. M. and Huang, D. (2017). New evidence shows that *Pocillopora* 'damicornis-like' corals in Singapore are actually *Pocillopora acuta* (Scleractinia: Pocilloporidae). *Biodivers. Data J.* 5, e11407. doi:10.3897/BDJ.5.e11407

- Putnam, H. M. and Edmunds, P. J. (2011). The physiological response of reef corals to diel fluctuations in seawater temperature. *J. Exp. Mar. Bio. Ecol.* 396, 216-223. doi:10.1016/j.jembe.2010.10.026
- Putnam, H. M. and Gates, R. D. (2015). Preconditioning in the reef-building coral Pocillopora damicomis and the potential for trans-generational acclimatization in coral larvae under future climate change conditions. J. Exp. Biol. 218, 2365-2372. doi:10.1242/jeb.123018
- Rädecker, N., Pogoreutz, C., Wild, C. and Voolstra, C. R. (2017). Stimulated respiration and net photosynthesis in *Cassiopeia* sp. during glucose enrichment suggests in hospite CO₂ limitation of algal endosymbionts. Front. Mar. Sci. 4, 2-5. doi:10.3389/fmars.2017.00267
- Rinkevich, B. (1989). The contribution of photosynthetic products to coral reproduction. *Mar. Biol.* **101**, 259-263. doi:10.1007/BF00391465
- Rodolfo-Metalpa, R., Hoogenboom, M. O., Rottier, C., Ramos-Esplá, A., Baker, A. C., Fine, M. and Ferrier-Pagès, C. (2014). Thermally tolerant corals have limited capacity to acclimatize to future warming. *Glob. Chang. Biol.* **20**, 3036-3049. doi:10.1111/gcb.12571
- Rodriguez-Casariego, J. A., Ladd, M. C., Shantz, A. A., Lopes, C., Cheema, M. S., Kim, B., Roberts, S. B., Fourqurean, J. W., Ausio, J., Burkepile, D. E. et al. (2018). Coral epigenetic responses to nutrient stress: Histone H2A.X phosphorylation dynamics and DNA methylation in the staghorn coral *Acropora cervicornis*. *Ecol. Evol.* 8, 12193-12207. doi:10.1002/ece3.4678
- Rogers, C. S. (1990). Responses of coral reefs and reef organisms to sedimentation. *Mar. Ecol. Prog. Ser.* 62, 185-202. doi:10.3354/meps062185
- Rohr, J. R., Civitello, D. J., Cohen, J. M., Roznik, E. A., Sinervo, B. and Dell, A. I. (2018). The complex drivers of thermal acclimation and breadth in ectotherms. *Ecol. Lett.* **21**, 1425-1439. doi:10.1111/ele.13107
- Rohwer, F., Seguritan, V., Azam, F. and Knowlton, N. (2002). Diversity and distribution of coral-associated bacteria. *Mar. Ecol. Prog. Ser.* **243**, 1-10. doi:10. 3354/meps243001
- Rosenberg, E. and Ben-haim, Y. (2002). Microbial diseases of corals and global warming. Environ. Microbiol. 4, 318-326. doi:10.1046/j.1462-2920.2002.00302.x
- Rosset, S., Wiedenmann, J., Reed, A. J. and D'Angelo, C. (2017). Phosphate deficiency promotes coral bleaching and is reflected by the ultrastructure of symbiotic dinoflagellates. *Mar. Pollut. Bull.* 118, 180-187. doi:10.1016/j. marpolbul.2017.02.044
- Schaum, C. E., Student Research Team, Ffrench-Constant, R., Lowe, C., Ólafsson, J. S., Padfield, D. and Yvon-Durocher, G. (2017). Temperaturedriven selection on metabolic traits increases the strength of an algal-grazer interaction in naturally warmed streams. *Glob. Chang. Biol.* 24, 1793-1803. doi:10. 1111/acb.14033
- Schmidt-Roach, S., Miller, K. J., Lundgren, P. and Andreakis, N. (2014). With eyes wide open: a revision of species within and closely related to the *Pocillopora damicornis* species complex (Scleractinia; Pocilloporidae) using morphology and genetics. *Zool. J. Linn. Soc.* 170, 1-33. doi:10.1111/zoj.12092
- Schoolfield, R. M., Sharpe, P. J. H. and Magnuson, C. E. (1981). Non-linear regression of biological temperature-dependent rate models based on absolute reaction-rate theory. J. Theor. Biol. 88, 719-731. doi:10.1016/0022-5193(81)90246-0
- Schulte, P. M., Healy, T. M. and Fangue, N. A. (2011). Thermal performance curves, phenotypic plasticity, and the time scales of temperature exposure. *Integr. Comp. Biol.* **51**, 691-702. doi:10.1093/icb/icr097
- Serrano, X. M., Miller, M. W., Hendee, J. C., Jensen, B. A., Gapayao, J. Z., Pasparakis, C., Grosell, M. and Baker, A. C. (2018). Effects of thermal stress and nitrate enrichment on the larval performance of two Caribbean reef corals. *Coral Reefs* 37, 173-182. doi:10.1007/s00338-017-1645-y
- Sgrò, C. M., Overgaard, J., Kristensen, T. N., Mitchell, K. A., Cockerell, F. E. and Hoffmann, A. A. (2010). A comprehensive assessment of geographic variation in heat tolerance and hardening capacity in populations of *Drosophila melanogaster* from Eastern Australia. *J. Evol. Biol.* 23, 2484-2493. doi:10.1111/j.1420-9101. 2010.02110.x
- Shantz, A. A. and Burkepile, D. E. (2014). Context-dependent effects of nutrient loading on the coral-algal mutualism. *Ecology*. 95, 1995-2005. doi:10.1890/13-1407.1
- **Sharpe, P. J. H. and Demichele, D. W.** (1977). Reaction kinetics of poikilotherm development. *J. Theor. Biol.* **64**, 649-670. doi:10.1016/0022-5193(77)90265-X
- Shea, F. and Watts, C. E. (1939). Dumas method for organic nitrogen. *Ind. Eng. Chem. Anal. Ed.* 51, 333-334. doi:10.1021/ac50134a013
- Silbiger, N. J., Guadayol, Ò., Thomas, F. I. M. and Donahue, M. J. (2014). Reefs shift from net accretion to net erosion along a natural environmental gradient. *Mar. Ecol. Prog. Ser.* 515, 33-44. doi:10.3354/meps10999
- Silbiger, N. J., Nelson, C. E., Remple, K., Sevilla, J. K., Quinlan, Z. A., Putnam, H. M., Fox, M. D. and Donahue, M. J. (2018). Nutrient pollution disrupts key ecosystem functions on coral reefs. *Proc. R. Soc. B. Biol. Sci.* 285, 20172718. doi:10.1098/rspb.2017.2718
- Silbiger, N. J., Goodbody-Gringley, G., Bruno, J. F. and Putnam, H. M. (2019). Comparative thermal performance of the reef-building coral *Orbicella franksi* at its latitudinal range limits. *Mar. Biol.* **166**, 126. doi:10.1007/s00227-019-3573-6

- Silverman, J., Lazar, B. and Erez, J. (2007). Community metabolism of a coral reef exposed to naturally varying dissolved inorganic nutrient loads. *Biogeochemistry* 84, 67-82. doi:10.1007/s10533-007-9075-5
- Sinclair, B. J., Williams, C. M. and Terblanche, J. S. (2012). Variation in thermal performance among insect populations. *Physiol. Biochem. Zool.* 85, 594-606. doi:10.1086/665388
- Sinclair, B. J., Marshall, K. E., Sewell, M. A., Levesque, D. L., Willett, C. S., Slotsbo, S., Dong, Y., Harley, C. D. G., Marshall, D. J., Helmuth, B. S. et al. (2016). Can we predict ectotherm responses to climate change using thermal performance curves and body temperatures? *Ecol. Lett.* 19, 1372-1385. doi:10. 1111/ele.12686
- Speare, K. E., Duran, A., Miller, M. W. and Burkepile, D. E. (2019). Sediment associated with algal turfs inhibits the settlement of two endangered coral species. *Mar. Pollut. Bull.* **144**, 189-195. doi:10.1016/j.marpolbul.2019.04.066
- Speers, A. E., Besedin, E. Y., Palardy, J. E. and Moore, C. (2016). Impacts of climate change and ocean acidification on coral reef fisheries: an integrated ecological-economic model. *Ecol. Econ.* 128, 33-43. doi:10.1016/j.ecolecon. 2016.04.012
- Stambler, N., Popper, N., Dubinsky, Z. and Stimson, J. (1991). Effects of nutrient enrichment and water motion on the coral *Pocillopora damicornis*. *Pacific Sci.* **45**, 299-307
- Stimson, J. and Kinzie, R. A. (1991). The temporal pattern and rate of release of zooxanthellae from the reef coral *Pocillopora damicornis* (Linnaeus) under nitrogen-enrichment and control conditions. *J. Exp. Mar. Biol. Ecol.* 153, 63-74. doi:10.1016/S0022-0981(05)80006-1
- Storlazzi, C. D., Field, M. E. and Bothner, M. H. (2011). The use (and misuse) of sediment traps in coral reef environments: theory, observations, and suggested protocols. *Coral Reefs* **30**, 23-38. doi:10.1007/s00338-010-0705-3
- Tattersall, G. J., Sinclair, B. J., Withers, P. C., Fields, P. A., Seebacher, F., Cooper, C. E. and Maloney, S. K. (2012). Coping with thermal challenges: physiological adaptations to environmental temperatures. *Compr. Physiol.* 2, 2151-2202. doi:10.1002/cphy.c110055
- Torres, A. F. and Ravago-Gotanco, R. (2018). Rarity of the "common" coral Pocillopora damicomis in the western Philippine archipelago. Coral Reefs 37, 1209-1216. doi:10.1007/s00338-018-1729-3
- Van Hooidonk, R., Maynard, J. A. and Planes, S. (2013). Temporary refugia for coral reefs in a warming world. *Nat. Clim. Chang.* 3, 508-511. doi:10.1038/ nclimate1829

- Van Woesik, R., Houk, P., Isechal, A. L., Idechong, J. W., Victor, S. and Golbuu, Y. (2012). Climate-change refugia in the sheltered bays of Palau: analogs of future reefs. *Ecol. Evol.* **2**, 2474-2484. doi:10.1002/ece3.363
- Veal, C. J., Carmi, M., Fine, M. and Hoegh-Guldberg, O. (2010). Increasing the accuracy of surface area estimation using single wax dipping of coral fragments. Coral Reefs 29, 893-897. doi:10.1007/s00338-010-0647-9
- Vega Thurber, R. L., Burkepile, D. E., Fuchs, C., Shantz, A. A., Mcminds, R. and Zaneveld, J. R. (2014). Chronic nutrient enrichment increases prevalence and severity of coral disease and bleaching. *Glob. Chang. Biol.* 20, 544-554. doi:10. 1111/gcb.12450
- Voolstra, C. R., Buitrago-López, C., Perna, G., Cárdenas, A., Hume, B. C. C., Rädecker, N. and Barshis, D. J. (2020). Standardized short-term acute heat stress assays resolve historical differences in coral thermotolerance across microhabitat reef sites. Glob. Chang. Biol. 26, 4328-4343. doi:10.1111/gcb.15148
- Wall, C. B., Mason, R. A. B., Ellis, W. R., Cunning, R. and Gates, R. D. (2017). Elevated pCO₂ affects tissue biomass composition, but not calcification, in a reef coral under two light regimes. R. Soc. Open Sci. 4, 170683. doi:10.1098/rsos.170683
- Wall, C. B., Ricci, C. A., Foulds, G. E., Mydlarz, L. D., Gates, R. D. and Putnam, H. M. (2018). The effects of environmental history and thermal stress on coral physiology and immunity. *Mar. Biol.* 165, 56. doi:10.1007/s00227-018-3317-z
- Wall, C. B., Ritson-Williams, R., Popp, B. N. and Gates, R. D. (2019). Spatial variation in the biochemical and isotopic composition of corals during bleaching and recovery. *Limnol. Oceanogr.* 64, 2011-2028. doi:10.1002/lno.11166
- Ward, S. (1995). Two patterns of energy allocation for growth, reproduction and lipid storage in the scleractinian coral *Pocillopora damicornis*. Coral Reefs 14, 87-90. doi:10.1007/BF00303428
- Weber, M., De Beer, D., Lott, C., Polerecky, L., Kohls, K., Abed, R. M. M., Ferdelman, T. G. and Fabricius, K. E. (2012). Mechanisms of damage to corals exposed to sedimentation. *Proc. Natl. Acad. Sci. USA* **109**, E1558-E1567. doi:10. 1073/pnas.1100715109
- Wiedenmann, J., D'Angelo, C., Smith, E. G., Hunt, A. N., Legiret, F.-E., Postle, A. D. and Achterberg, E. P. (2013). Nutrient enrichment can increase the susceptibility of reef corals to bleaching. *Nat. Clim. Chang.* 3, 160-164. doi:10. 1038/nclimate1661
- **Wooldridge, S. A.** (2009). Water quality and coral bleaching thresholds: formalising the linkage for the inshore reefs of the Great Barrier Reef, Australia. *Mar. Pollut. Bull.* **58**, 745-751. doi:10.1016/j.marpolbul.2008.12.013

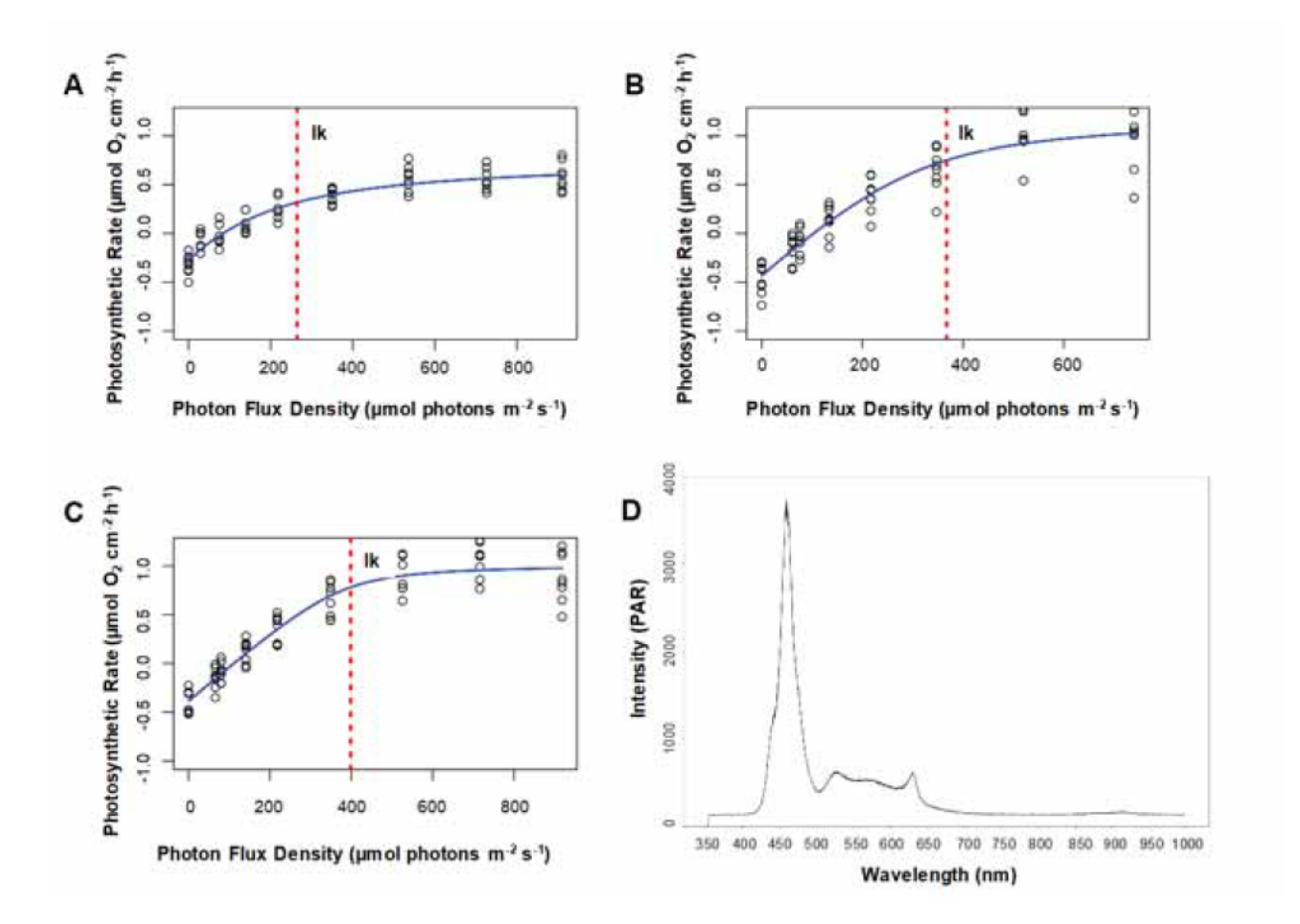


Figure S1. Photosynthesis - photon flux density curves (also known as photosynthesis-irradiance curves) characterized for (n=8) *P. acuta* fragments collected from the A. eastern, B. central, and C. western sites on the north shore fringing reef of Mo'orea, French Polynesia. A. Light saturation point ($I_k = 264.48 \mu mol photons m^2 s^{-1}$), B. ($I_k = 367.43 \mu mol photons m^2 s^{-1}$), C. ($I_k = 398.47 \mu mol photons m^2 s^{-1}$) is indicated by the dashed red line. D. Spectral trace of Mars Aqua 300w LED Brand Epistar light during experimental trials.

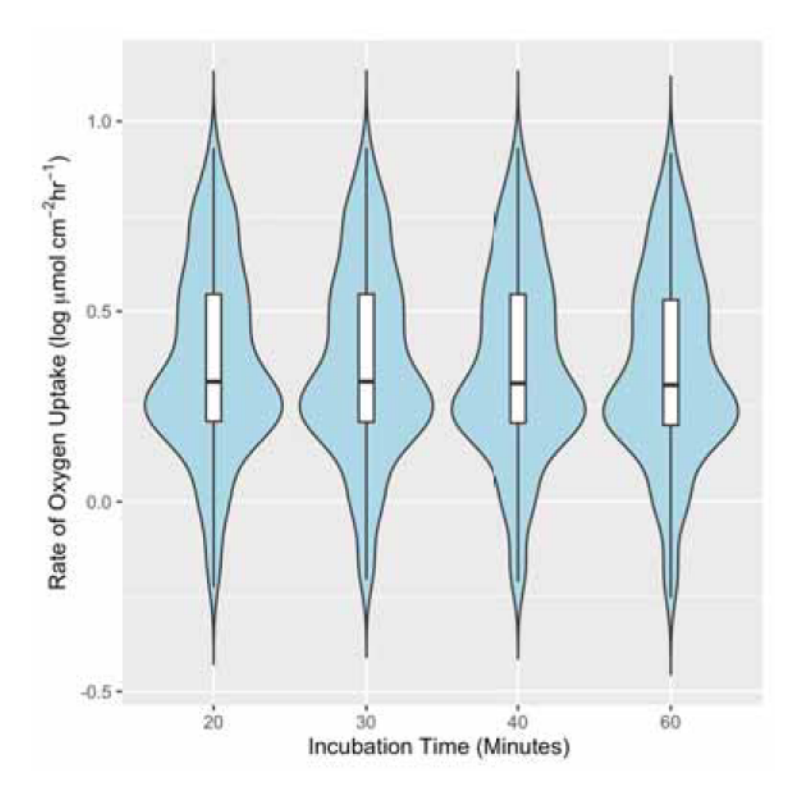


Figure S2. Violin plots filled with boxplots summarizing the distribution of values for respiration rates measured at four different incubation times. Data were collected in January 2019 (n=16).

Mo'orea, French Polynesia.

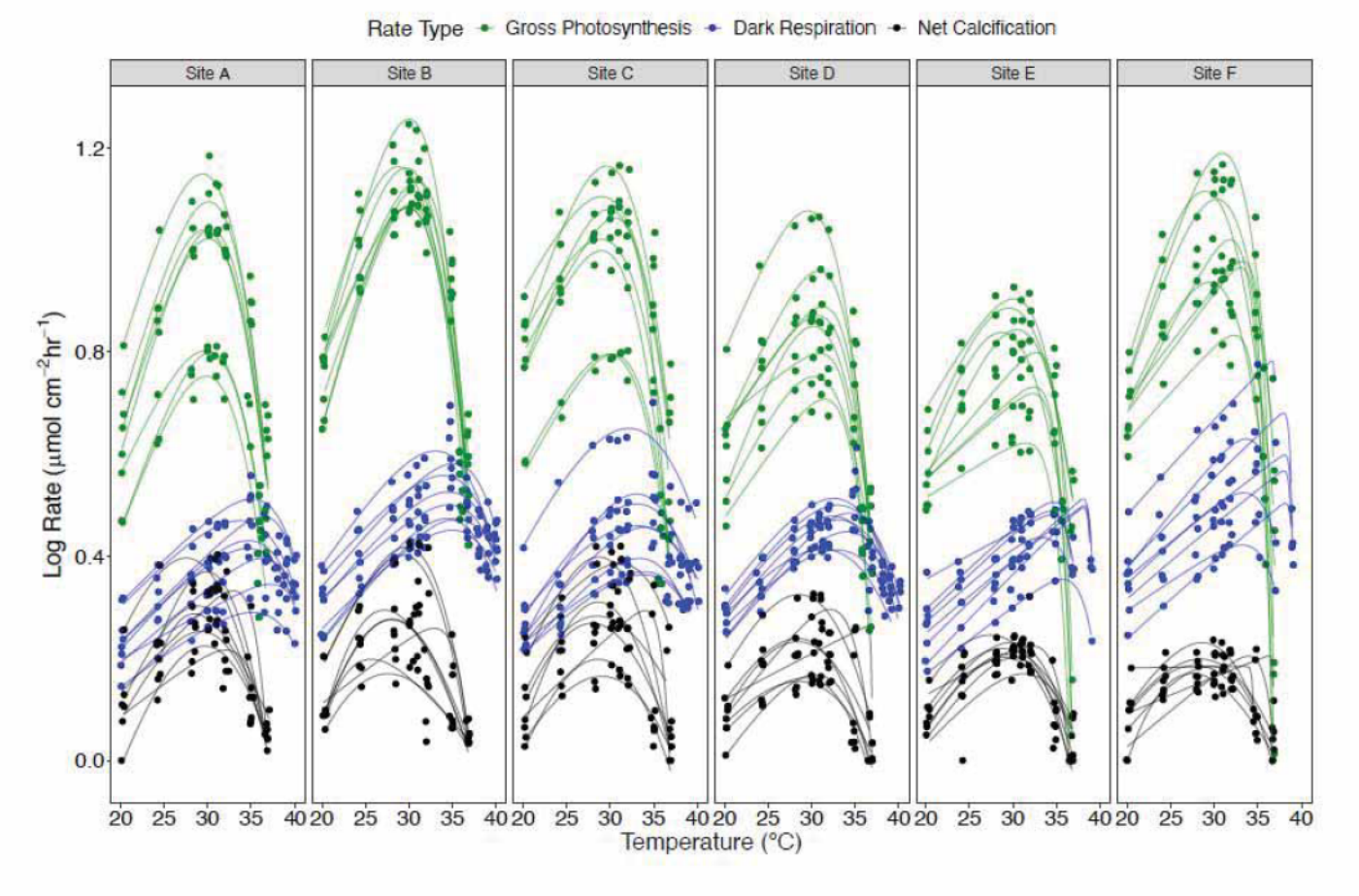


Figure S3. Thermal performance curves (TPCs) of log (x + 1) gross photosynthetic (green), dark respiration (blue), and net calcification (black) rates (μ mol cm⁻² hr⁻¹) from *P. acuta* fragments (n = 48) at each of the six north shore fringing reef sites in

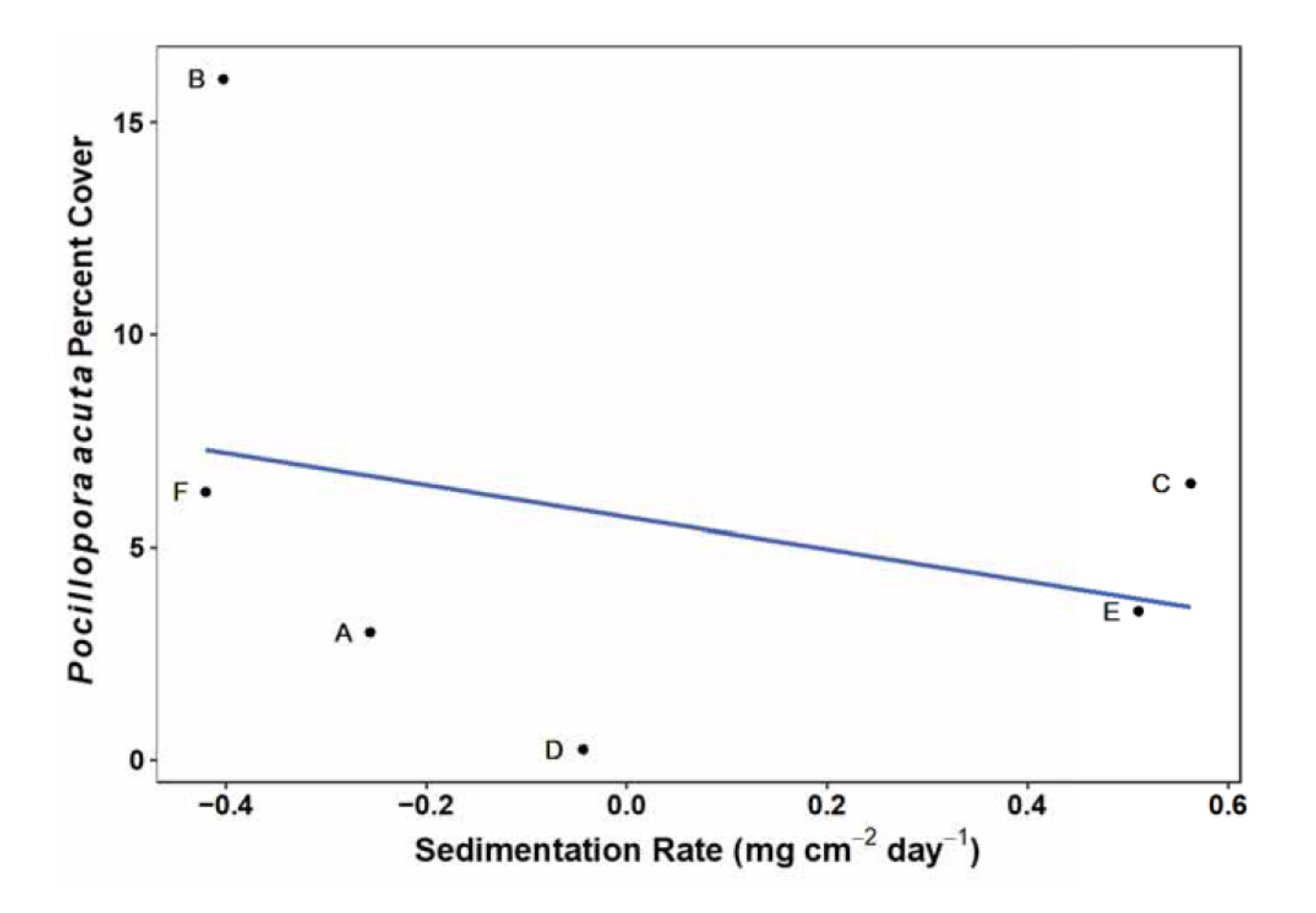


Figure S4. Linear regression of *P. acuta* percent cover as a function of sedimentation rate residuals (mg cm⁻² day⁻¹) (n = 6) ($r^2 = 0.10$, p < 0.001). Each dot is the percent cover from an individual site (A-F) along the north shore fringing reef of Mo'orea, French Polynesia and the blue line is the best fit line with 95 % CI.

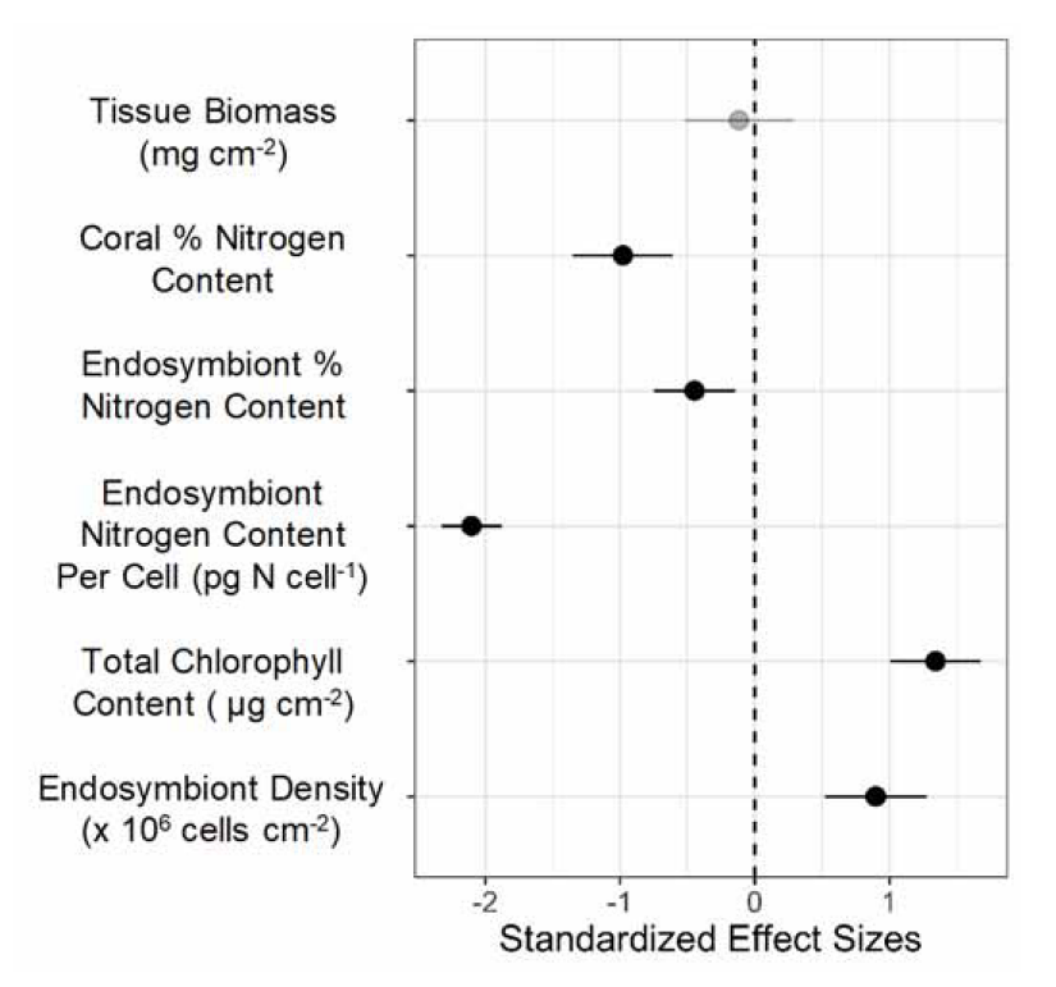


Figure S5. Standardized effect sizes from individual mixed effects models for endosymbiont and coral response variables as a function of sedimentation rate (mg cm $^{-2}$ day $^{-1}$) residuals (n = 54). Values are effect sizes \pm 95% CI. All response variables were standardized and values with 95% CI that do not cross zero are considered statistically significant (see Table S1B). The light grey/transparent variables are not statistically significant.

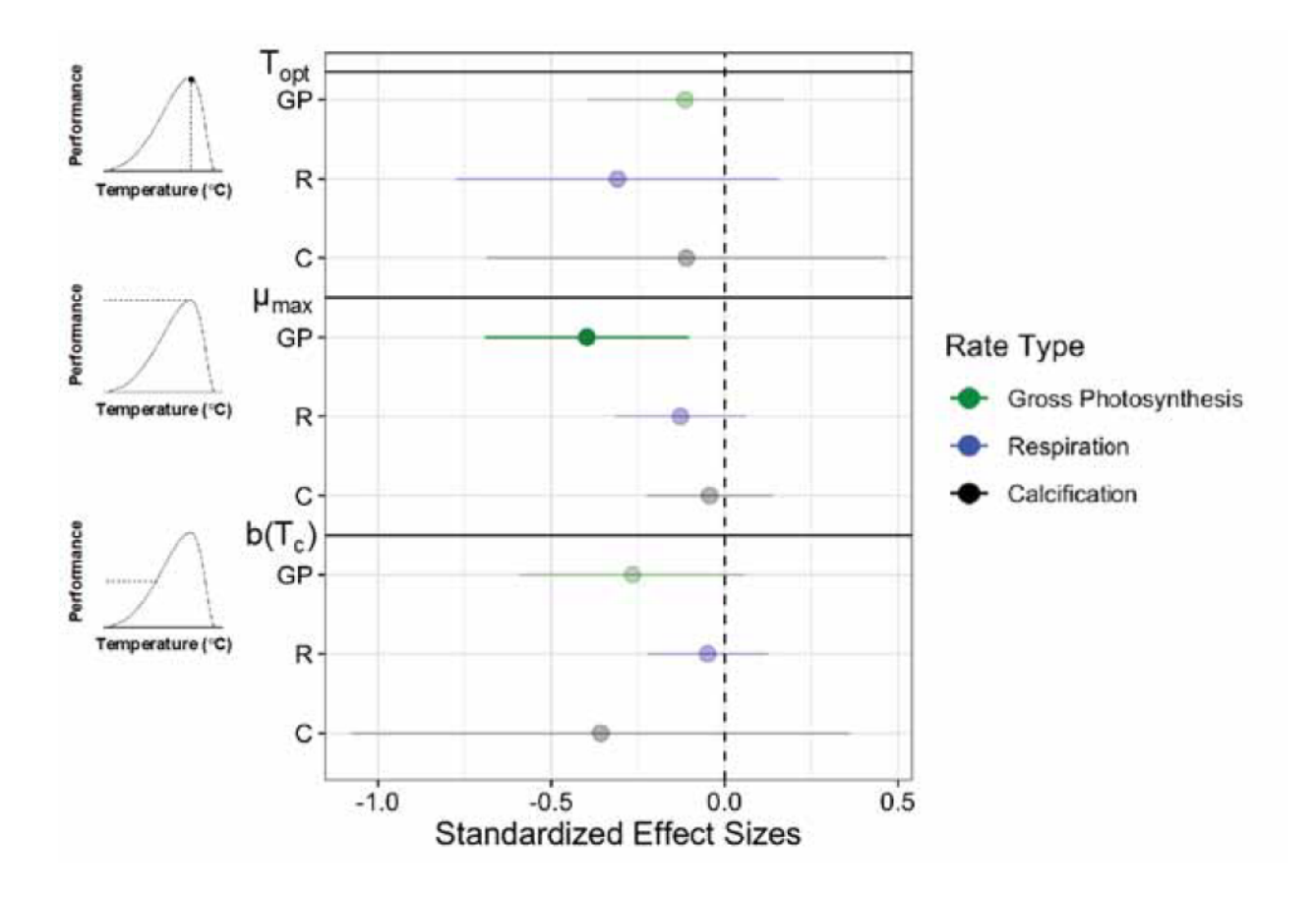


Figure S6. Standardized effect sizes from individual mixed effects models for thermal performance metrics as a function of sedimentation rate (mg cm $^{-2}$ day $^{-1}$) residuals (n = 48). Values are effect sizes \pm 95% CI. 95% CI that do not cross zero are considered statistically significant (see Table S3A, B, and C) .

Table S1: A. Table displaying the statistical results for all coral and endosymbiont response variables by % N residual models **B.** Table displaying the statistical results for all coral and endosymbiont response variables by sedimentation rate residual models. Bold p-values are significant at the $\alpha < 0.05$ level. 95% confidence interval values are shown in parentheses.

Α.	Endosymbiont Density		Chlorophyll a Content		Tissue Biomass		Coral % N Content		Endosymbiont N Content Per Cell		Endosymbiont % N Content	
Predictors	Estimate s	P-Value	Estimates	P-Value	Estimates	P-Value	Estimates	P- Value	Estimates	P-Value	Estimates	P-Value
Intercept	1.07 (0.78 – 1.37)	<0.001	6.55 (3.97 – 9.12)	<0.001	8.67 (8.24 – 9.10)	<0.001	21.71 (21.05 – 22.38)	<0.001	5.04 (4.72 – 5. 36)	<0.001	16.50 (14.55 – 18.46)	<0.001
% Nitrogen Content Residuals	2.93 (1.81 – 4.06)	<0.001	23.62 (16.44 - 30.80)	<0.001	4.14 (- 3.08 – 11.35)	0.261	6.76 (-0.36 - 13.88)	0.063	-5.45 (-7.50 3.39)	<0.001	6.64 (4.00 – 9.28)	<0.001
Random Effec	ts											
σ^2	0.13		5.42		6.77		5.76		0.45		0.73	
T00	0.04 site		3.38 site		0.00 atu		0.15 site		0.05 site		1.98 and	
ICC	0.25		0.38				0.03		0.09		0.73	
N	2 one		2		2 site		2 site		2 sine		2 sine	
Observations	141		141		141		141		141		141	
Marginal R ² / Conditional R ²	0.148/0	357	0.185 / 0.498		0,009 / NA		0.027 / 0.051		0.174 / 0.23	53	0.055 / 0.7	45

В.	Endosymbiont Density		Chlorophyll a Content		Tissue Biomass		Coral % N Content		Endosymbiont N Content Per Cell		Endosymbiont % N Content	
Predictors	Estimates	P-Value	Estimates	P-Value	Estimates	P-Value	Estimates	P-Value	Estimates	P-Value	Estimates	P-Value
Intercept	1.07 (0.88 – 1.26)	<0,001	6.54 (4.68 – 8.40)	<0.001	8.67 (8.24 – 9.10)	<0.001	21.71 (20.38 – 23.03)	<0.001	5.04 (4.79 – 5.29)	<0.001	16.50 (14.97 – 18.03)	<0.001
Sedimentation Rate Residuals	0.36 (0.21 – 0.52)	<0.001	3.67 (2.75 – 4.58)	<0.001	-0.30 (- 1.37 – 0.76)	0.576	-2.40 (-3.32 1.49)	<0.001	-1.54 (-1.71 1.38)	<0.001	-0.55 (-0.92 0.18)	0.004
Random Effect	ts											
σ^2	0.14		4.88		6.82		4.90		0.16		0.81	
T00	0.02 site		1.73 site		0.00 site		0.85 see		0.03 _{site}		1.21 ste	
ICC	0.11		0.26				0.15		0.16		0.60	
N	2 site		2 site		2 site		2 site		2 site		2 site	
Observations	141		141		141		141		141		141	
Marginal R ² / Conditional R ²	0.123 / 0.	222	0.251 / 0.448		0.002 / NA		0.142 / 0.2	69	0.675 / 0.729		0.024 / 0.60	8

Table S2: A. Table displaying the statistical results for all T_{opt} **B.** μ max, and **C.** $b(T_c)$ by % N residual models. Bold p-values are significant at the $\alpha < 0.05$ level. 95% confidence interval values are shown in parentheses.

A	Topt_C	SP.	Topt_	R	Topt_C		
Predictors	Estimates	P-Value	Estimates	P-Value	Estimates	P-Value	
Intercept	30.43 (30.11 – 30.75)	<0.001	34.66 (33.82 – 35.50)	<0.001	29.84 (29.19 – 30.50)	<0.001	
% Nitrogen Content Residuals	0.17 (-5.24 – 5.57)	0.951	-13.34 (-22.20 – -4.47)	0.003	1.93 (-9.07 – 12.93)	0.731	
Random Effects							
σ^2	1.27		2.97		5.25		
T00	0.00 site		0.24 site		0.00 site		
ICC			0.07				
N	2 site		2 site		2 site		
Observations	47	9	47		47		
Marginal R ² / Conditional R ²	0.000 / 0.000		0.167 / 0.229		0.003 / 0.003		
В	μта	_GP	μma	x_R	μma	c_C	
Predictors	Estimates	P-Value	Estimates	P-Value	Estimates	P-Value	
Intercept	0.99 (0.87 – 1.11)	<0.001	0.50 (0.43 – 0.57)	<0.001	0.29 (0.26 - 0.31)	<0.001	
% Nitrogen Content Residuals	-1.05 (-1.74 – -0.37)	0.002	-0.12 (-0.57 – 0.32)	0.587	-0.34 (-0.72 - 0.04)	0.080	
Random Effects							
σ^2	0.02		0.01		0.01		
T00	0.01 site		0.00 site		0.00 site		
ICC	0.29		0.21				
N ·	2 site		2 site		2 site		
Observations	47		47		47		
Marginal R2 / Conditional R2	0.146 / 0.398		0.006 / 0.219		0.063 / 0.063		
C	b(T _c)	b(T _c)_GP		_R	b(T _c)_C		
Predictors	Estimates	P-Value	Estimates	P-Value	Estimates	P-Value	
Intercept	0.94 (0.82 - 1.05)	<0.001	0.41 (0.33 – 0.49)	<0.001	0.45 (0.36 - 0.54)	<0.001	
% Nitrogen Content Residuals	-0.91 (-1.67 – -0.15)	0.019	0.21 (-0.20 - 0.62)	0.322	-1.70 (-3.24 – -0.15)	0.031	
Random Effects							
σ^2	0.02		0.01		0.10		
T00	0.01 sac		0.00 site		0.00 site		
ICC	0.23		0.34				
N	2 site		2 site		2 sinc		
Observations	47		47		47		
Marginal R ² / Conditional R ²	0.100 / 0.307		0.017 / 0.349		0.091 / 0.091		

Table S3: A. Table displaying the statistical results for all T_{opt} **B.** μ max, and **C.** $b(T_c)$ by sedimentation rate residual models. Bold p-values are significant at the $\alpha < 0.05$ level. 95% confidence interval values are shown in parentheses.

A	Topt_GI	•	Topt_R	Ł	Topt_C		
Predictors	Estimates	P-Value	Estimates	P-Value	Estimates	P-Value	
Intercept	30.43 (30.11 – 30.75)	<0.001	34.66 (34.14 – 35.19)	<0.001	29.84 (29.19 – 30.50)	<0.001	
Sedimentation Rate Residuals	-0.32 (-1.11 – 0.47)	0.426	-0.87 (-2.17 – 0.44)	0.193	-0.31 (-1.93 – 1.31)	0.707	
Random Effects							
σ^2	1.25		3.42	á	5.25		
T00	0.00 site		0.00 site		0.00 site		
N	2 site		2 site		2 site		
Observations	47		47	9	47		
Marginal R2 / Conditional R2	0.014 / 0.014		0.036 / 0.036		0.003 / 0.003		
В.	μтах	_GP	μms	ıx_R	μта	x_C	
Predictors	Estimates	P-Vali	ue Estimates	P-Value	e Estimates	P-Value	
Intercept	0.99 (0.83 – 1.15)	<0.00	1 0.50 (0.43 – 0.57)	<0.001	0.29 (0.26 - 0.31)	<0.001	
Sedimentation Rate Residuals	-0.13 (-0.22 – -0.03)	0.008	-0.04 (-0.10 – 0.02	0.184	-0.01 (-0.07 – 0.04)	0.643	
Random Effects							
σ^2	0.02		0.01		0.01		
Т00	0.01 site		0.00 site		0.00 site		
ICC	0.42		0.22				
N	2 site		2 site		2 site		
Observations	47		47		47		
Marginal R2 / Conditional R2	0.084 / 0.464		0.030 / 0.243		0.005 / 0.005		
C	b(T _c)_	b(T _c)_GP b(T _c)			_R b(T _c)		
Predictors	Estimates	P-Valu	e Estimates	P-Value	Estimates	P-Value	
Intercept	0.94 (0.79 – 1.09)	<0.001	0.41 (0.34 – 0.47)	<0.001	0.45 (0.32 - 0.58)	<0.001	
Sedimentation Rate Residuals	-0.09 (-0.19 – 0.02)	0.108	-0.02 (-0.07 – 0.04)	0.576	-0.12 (-0.35 – 0.12)	0.331	
Random Effects							
σ^2	0.02		0.01		0.11		
T00	0.01 site		0.00 site		0.00 site		
ICC	0.33		0.25		0.03		
N	2 site		2 site		2 site		
Observations	47		47		47		
Marginal R^2 / Conditional R^2	0.037 / 0.357		0.005 / 0.252		0.020 / 0.054		